CHALMERS
UNIVERSITY OF TECHNOLOGY

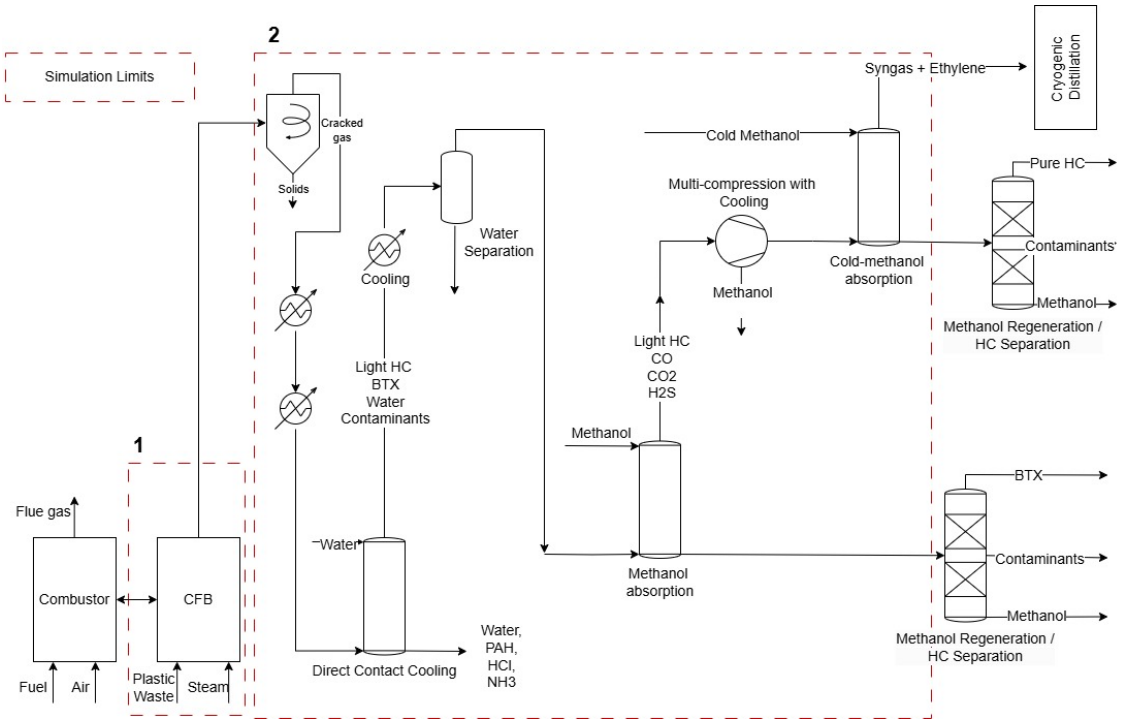

Fractionation of Cracker Effluent from Steam Cracking of Plastic Waste

Process Modeling of Methanol-Based Scrubber-Distillation System

Master's thesis in Innovative and Sustainable Chemical Engineering

LUIS ENRIQUE ANAYA AGUILAR

DEPARTMENT OF EARTH, SPACE AND ENVIRONMENT

CHALMERS UNIVERSITY OF TECHNOLOGY
Gothenburg, Sweden 2025
www.chalmers.se

Master's thesis 2025

Fractionation of Cracker Effluent from Steam Cracking of Plastic Waste

Process Modeling of Methanol-Based Scrubber-Distillation System

LUIS ENRIQUE ANAYA AGUILAR

CHALMERS
UNIVERSITY OF TECHNOLOGY

Department of Earth, Space and Environment
Division of Energy Technology
Chalmers University of Technology
Gothenburg, Sweden 2025

Fractionation of Cracker Effluent from Steam Cracking of Plastic Waste
Process Modeling of Methanol-Based Scrubber-Distillation System
LUIS ENRIQUE ANAYA AGUILAR

© LUIS ENRIQUE ANAYA AGUILAR, 2025.

Supervisor: Chahat Mandviwala, Energy Technology Division
Supervisor: Judit Fortet, Energy Technology Division
Examiner: Martin Seemann, Energy Technology Division

Master's Thesis 2025
Department of Earth, Space and Environment
Division of Energy Technology

Chalmers University of Technology
SE-412 96 Gothenburg
Telephone +46 31 772 1000

Typeset in LaTeX
Printed by Chalmers Reproservice
Gothenburg, Sweden 2025

Fractionation of Cracker Effluent from Steam Cracking of Plastic Waste
Process Modeling of Methanol-Based Scrubber-Distillation System
LUIS ENRIQUE ANAYA AGUILAR
Department of Earth, Space, and Environment
Chalmers University of Technology

Abstract

Plastic waste presents a major management problem, as most plastics are disposable and end up either being incinerated, in a landfill, or mechanically recycled while loosing mechanical properties. The use of chemical recycling technologies, such as plastic waste steam cracking, presents an alternative to conventional recycling, as well as to typical hydrocarbon cracking processes. However, adjustments to the gas cleaning and separation processes need to be done to implement these technologies into existing chemical clusters. This work presents the evaluation of a new cleaning and separation process based on water scrubbing and methanol absorption to remove acid gases (NH_3, HCl, H_2S, CO_2) and separate valuable compounds (aromatics, olefins), to understand the feasibility of implementing this technology together with plastic waste steam cracking. ASPEN Plus V.14. was used to simulate the process, with the main output from the software being removal efficiencies, equipment sizing, and energy requirements. Water scrubbing proved to be the best option to remove HCl and NH_3 from the cracked gas stream, while also condensing PAH. A multi-stage compressor increasing pressure from 1 to 33 bar can condense aromatics, removing benzene by 90% while preparing the cold methanol absorber feed. Ethylene needs high methanol flowrates (4000 kg/ton MPW) to be fully absorbed in methanol at the operating conditions. Minimizing methanol use while removing contaminants will lead to approximately 50% of ethylene being absorbed. Methanol regeneration presents a major challenge, as an azeotrope is formed between ethylene and CO_2. Olefin production cost ranges from 6 to 10 SEK/ kg olefin produced. Methanol absorption has been proven to be a feasible option when cleaning acid gases. However, both BTXS and olefin absorption present challenges such as high methanol demand and regeneration challenges due to the azeotropic nature of the methanol-rich streams.

Keywords: plastic, methanol, cracking, ethylene, propylene, absorption, olefin, aromatics, methanol-absorption.

Acknowledgements

I would like to thank both of my supervisors Judit and Chahat for discussing the thesis topics with me, always giving relevant input and being interested in the project, as well as the gasification group and my examiner Martin for listening and always being open to any question I had throughout the thesis period. I would also like to thank my family, specially my parents, for giving me the opportunities that led me to this point in my life.

Luis Enrique Anaya Aguilar, Gothenburg, June 2025

List of Acronyms

Below is the list of acronyms that have been used throughout this thesis listed in alphabetical order:

BTXS	Benzene, Toluene, Xylene, Styrene
CAPEX	Capital Expenditures
CFB	Circulating Fluidized Bed
DCC	Direct Contact Cooling
DFB	Dual Fluidized Bed
ISBL	Inside Battery Limits
LPG	Liquefied Petroleum Gas
MPW	Mixed Packaging/Plastic Waste
Mt	Million Metric Tons
OPEX	Operational Expenditures
PC-SAFT	Perturbed Chain – Statistical Associating Fluid Theory
PE	Poly-Ethylene
PENG-ROB	Peng–Robinson Equation of State
PSRK	Predictive Redlich-Kwong-Soave equation of state
PVC	Polyvinyl chloride
RK-ASPEN	Redlich–Kwong Equation of State

Nomenclature

Below is the nomenclature of indices, sets, parameters, and variables that have been used throughout this thesis.

Variables

H_2	Hydrogen
H_2O	Water
CO	Carbon monoxide
CO_2	Carbon dioxide
CH_4	Methane
C_2H_4	Ethylene
C_2H_6	Ethane
C_3H_6	Propylene
C_3H_8	Propane
C_4H_6	1,3-Butadiene
C_4H_8	1-Butene
C_4H_8	Isobutylene
C_5H_{12}	C5Hx
C_6H_6	Benzene
C_7H_8	Toluene
C_8H_{10}	Xylenes
$C_{10}H_8$	PAHs
C	Solid Carbon
H_2O	Water
H_2S	Hydrogen sulfide
NH_3	Ammonia
HCl	Chloridric acid

Contents

List of Figures

List of Tables

1

Introduction

Plastics are present in different manufacturing sectors, with primary applications in packaging, consumer products, textiles, electronics, transportation, machinery, and construction. Geyer et al. [1] estimated that 8,300 million metric tons (Mt) of virgin plastic had been produced globally by 2015. In 2019, 353 Mt of plastic waste had been generated, with only 9% of it being recycled [2]. Global plastic production increased by 12% between 2018 and 2023, reaching 414 Mt in 2023, of which 90.4% originate from fossil fuels, 8.9% from post-consumer mechanical recycling, and less than 0.1% from chemical recycling [3]. In contrast, European plastic production decreased by 13% during the same period, 79.4% being derived from fossil fuels, 19% from mechanical recycling, 1.4% from bio-based feedstocks, and less than 0.2% from chemical recycling [3]. The inexpensive manufacturing of plastics, attributed to their reliance on fossil feedstocks, accounts for 4 to 6% of global fossil fuel consumption, minimizing concerns about resource depletion. However, their persistence in the environment post-disposal creates significant challenges in waste management [4]. To address these challenges, advanced processes and technologies are required to transition from a linear model, where plastic is produced from fossil sources, to a circular economy that prioritizes reuse and recycling.

Conventional plastic production is based on light olefins derived from the cracking process of fossil fuels. Light olefins, unsaturated hydrocarbons, include ethylene, propylene, butenes, and butadiene. These compounds serve as the major building blocks of the chemical industry, with ethylene and propylene being the key monomers used for plastic production, such as polyethylene, polyvinyl chloride (PVC), polypropylene and acrylonitrile [5]. The demand for olefins has increased steadily, reaching approximately 250 Mt in 2022 [6]. The production of olefin through steam cracking can use either liquid (naphtha) or gaseous (LPG, ethane) feedstocks and is divided into four main sections: the cracking furnace, quench section, compression and condensate section for acid gas removal, and separation columns for fractionation. The final products after the downstream process (gas cleaning and separation) go from heavy fuel oil and aromatics, to olefin compounds such as ethylene, propylene, and butadiene.

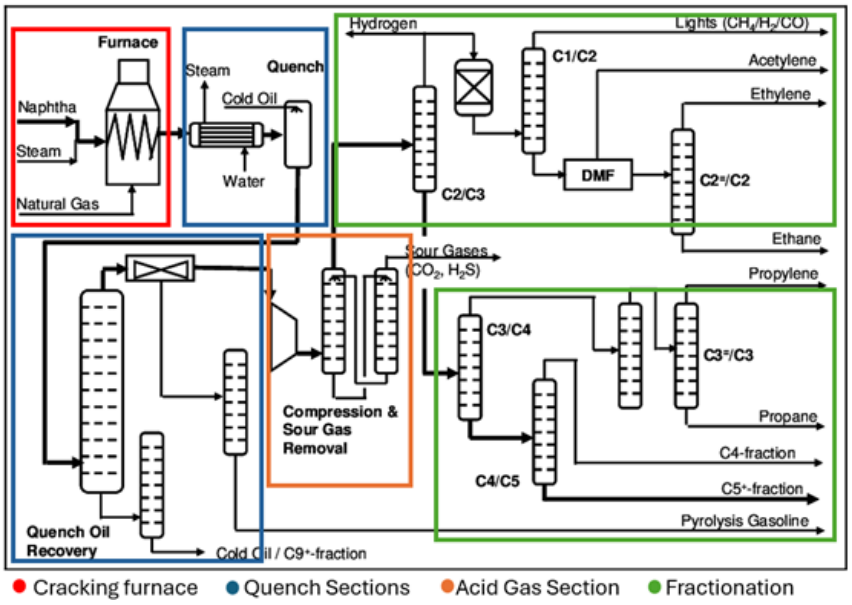

Figure 1.1: Simplified diagram of a naphtha cracker, adapted from [7]

Figure 1.1 shows a simplified naphtha cracking process. The feedstock enters the furnace together with steam at high temperatures (750–850°C) to promote thermal cracking, breaking down larger hydrocarbon molecules into smaller ones. The gas from the furnace then enters the quench section, where it is cooled to stop further reactions using water and cold oil. Next, the gases are compressed and passed through a gas removal system to eliminate sour gases such as CO_2 and H_2S. Finally, the separation and fractionation units isolate the gaseous mixture based on boiling points, producing products such as ethylene, propylene, hydrogen, fractions C4 and C5, and pyrolysis gasoline [7]. These products are further used as raw materials for plastic production.

Plastic products have an average lifespan of 10 years. However, packaging, consumer, and textile products have a shelf life of 0.5, 3, and 5 years, respectively [1]. If current trends in production and waste management persist, an estimated 12,000 Mt of plastic waste could accumulate in the environment by 2050 [1]. Plastic waste streams can be used both as a source of energy recovery and recycling. Recycling approaches are categorized into four types: primary, secondary, tertiary, and quaternary. Primary recycling involves the re-use of uncontaminated plastic scrap. Secondary or mechanical recycling involves cleaning, melting, and remolding plastics into new forms. Tertiary or feedstock recycling refers to thermochemical processes that break down long-chain hydrocarbon polymers into monomers and shorter-chain oligomers. Quaternary recycling involves incineration and the generation of energy from waste [8]. Waste-to-energy technologies have been widely adopted but face environmental challenges, such as the production of toxic gases and heavy-metal-contaminated ash [8]. The success of recycling depends on several factors, including recycling technologies, segregation techniques, pollutant and impurity removal, and sorting procedures [9]. Mechanical recycling, while widely used, has limitations in

the production of high-quality materials and can only be applied a finite number of times [10]. In Europe, mechanically recycled plastics accounted for 19% of total plastic production in 2023, compared to only 8.7% globally [3].

The transition from linear to circular plastic use requires technologies capable of processing diverse plastic waste streams and converting them into new plastics without material degradation. Thermochemical recycling addresses this challenge by recovering the molecular building blocks of plastics, serving as a bridge between plastic waste and new applications [4]. Companies such as British Petroleum and Eastman have initiated projects to implement tertiary recycling processes for the production of high quality plastics [8], as pyrolytic oil and gas products derived from plastic waste can help reduce the dependence on fossil fuels [9].

The direct cracking of feedstock to olefin and aromatics is favorable due to the process simplification, as units such as dehydrogenation or reforming are not needed, reducing the CAPEX and OPEX of the process. Different technologies, such as pyrolysis, catalytic cracking, and gasification show potential for recycling plastic waste, being the main challenge the inadequacy of actual steam crackers to directly use plastic waste [10]. A more robust reactor is needed to operate the process, capable of handling solid and liquid feedstock.

The steam cracking of MPW in a dual fluidized bed (DFB) reactor has demonstrated yields of methane, ethylene, propylene, and C_4 olefins comparable to those of conventional steam cracking of naphtha. This process achieves a 52% yield from polyolefin into light olefin and more than 15% aromatic yield when using a pure polyolefin feedstock [10]. The DFB plastic waste steam cracking process could offer petrochemical clusters the opportunity to transition to thermochemical recycling plants by replacing conventional steam crackers with DFB reactors. This approach allows for the use of various feedstocks, such as contaminated streams, liquid or solid feedstock, and a longer range of hydrocarbons [10].

Compared to a typical naphtha cracking furnace (tubular reactor), the DFB system is capable of using solid feedstock, not possible to use in regular naphtha crackers due to their tubular design [10]. Similarities and differences in DFB and conventional steam cracking (products).

As the product distributions from both steam cracking methods are similar, existing gas separation units do not require replacement. However, additional downstream cleaning processes may be necessary to address high concentrations of contaminants such as NH_3, H_2S,HCl, and CO_x [10] due to the elemental composition of the feedstock, containing nitrogen, chloride, and sulfur. If present in the downstream process, these contaminants would cause corrosion, catalyst poisoning, fouling, and toxicity and safety risks. Revamping conventional steam cracker effluent processing is essential to obtain high-purity monomers for the production of new plastic products.

Gas purification technologies, such as water scrubbing and methanol absorption,

can target these contaminants [11], removing them from the cracked gas stream. Methanol scrubbing shows potential for BTXS and olefin absorption due to its inherent absorption properties at low temperatures and high pressures [12].

A gas purification system must be developed to separate contaminants coming from the steam cracking of solid feedstock in a DFB system, while also targeting the separation of valuable components as aromatics and olefins.

1.1 Aim and scope

This study aims to identify the optimal process parameters, design specifications, and feasibility of using a cold methanol scrubbing-distillation system for the separation of the outlet stream from plastic waste steam cracking. The work focuses on the purification and recovery of light-olefins and aromatics, the challenges associated with methanol regeneration and hydrocarbon separation, and the effect of contaminants such as CO_x, H_2S, HCl, and NH_3 in the effluent stream. By modeling the separation processes in Aspen Plus V14 and doing an economic analysis, the operational feasibility and production price range for olefins with DFB technology and cold methanol scrubbing system for contaminant removal will be determined.

Research questions:

- What are the optimal design and operating conditions for a methanol-based scrubber and distillation system to effectively separate hydrocarbons from cracker effluent derived from plastic waste steam cracking?
- How effective is methanol as an absorption medium for capturing and purifying light olefins and BTXS from cracker effluent, and what challenges are associated with methanol regeneration?
- How do variations in the composition of cracker effluent, such as increased levels of CO_x, H_2S, HCl, and NH_3 impact the performance and efficiency of the separation and purification process?

1.2 Limitations

The following limitations were encountered when analyzing the scope and limits of the project:

- No experimental data is available to verify the modeling results. Because of this, data adapted from the reviewed literature could be used to compare the obtained results in the model.
- As an innovative process, no data is available in current literature. The model will focus on analyzing the feasibility of using cold methanol absorption for the steam cracking effluent purification. Lab tests should be included in a future

research to validate the process model.

- Methanol regeneration and distillation processes are not simulated due to time constrains.
- The techno-economic analysis done in this project is just an approximation to reality, since not all energy and equipment required is considered.

2

Literature Review

In this chapter, relevant topics for process design will be analyzed and discussed. Starting with the actual plastic production process, plastic waste management, thermochemical conversion of plastic waste, methanol absorption systems, and a proposed process to model.

2.1 Plastic production process

An analysis of an actual naphtha cracking process for ethylene production is studied. An average production plant can produce approximately 600 kton ethylene/ year [13]. Assuming 9 crackers involved in the operation, working with different raw materials such as ethane, propane, naphtha, and butane [14].

Figure 2.1 shows an industrial naphtha cracking process [14], where the feedstock enters the cracking furnace together with steam at approximately 850°C. The hot gases are then quenched with liquid oil to avoid any further reactions, reaching a temperature of approximately 200°C. The cold gas then enters a primary fractionator where heavy (C_9+) and light fractions are separated, further cooling is required to separate water in a drum. The light gas stream then undergoes compression (with hydrocarbon liquefaction and separation), directed into a caustic tower to remove acid gases such as H_2S and CO_2. Next, the cracked stream goes to the fractionation process, where olefins are separated in different distillation processes. Table A.1 shows the product composition of a typical naphtha cracking process. Traces of contaminants might be present in the feedstock due to its quality. However, there is not a significant amount for them to be removed.

2.2 Distillation techniques for hydrocarbon separation

Light olefin separation technologies are among the most energy-intensive petrochemical processes due to the similar molecular sizes and close relative volatility of the components being separated (e.g., olefins and paraffins) [15]. Traditional separation methods such as distillation and extraction have been industrially implemented. However, these techniques suffer from high energy demands and low separation

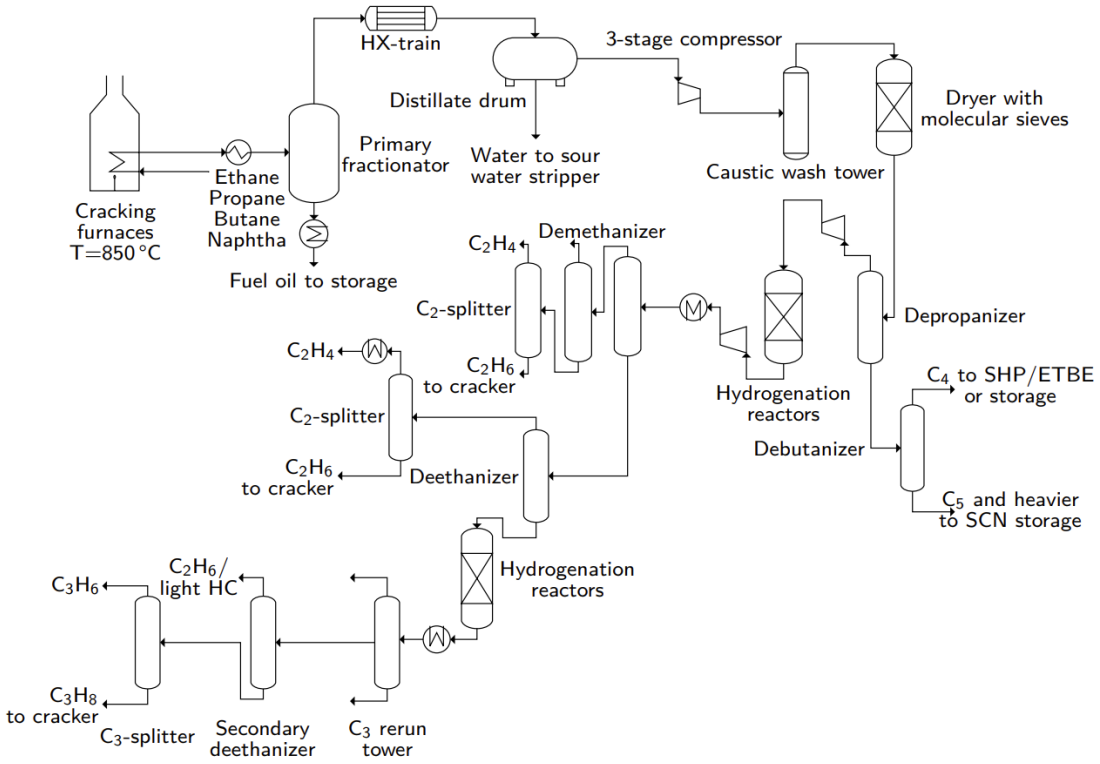

Figure 2.1: Borealis Steam Cracking Process Flow Diagram. From [14]

efficiency [16]. Current separation technologies are not equipped to handle high amounts of carbon oxides and acid gases, as conventional naphtha cracking produces negligible concentrations of these contaminants [10]. Furthermore, CO_2 must be removed prior to the separation unit to prevent freezing at low temperatures or absorption into the ethylene stream [17]. Corrosion remains a critical challenge in hydrocarbon production, posing risks to operational safety and facility integrity. Mixtures of H_2S and CO_2 are particularly corrosive and damaging if they reach sensitive areas of the process [18].

Figure 2.2 illustrates a traditional cryogenic olefin separation process, which operates at temperatures of 183–258 K, pressures of 7–28 bar, and requires over 100 trays with specific reflux ratios to meet ethylene and propylene purity standards. In this process, the hydrocarbon feed is first directed to the de-ethanizer, where ethane (C_2) and lighter gases are separated from heavier hydrocarbons. The C_2 stream is then fed to the C_2 splitter to isolate ethylene, ethane, and light gases. The heavier hydrocarbons from the de-ethanizer proceed to the de-propanizer, separating C_3 compounds from C_4 compounds. Finally, the C_3 splitter isolates propylene from propane.

Figure 2.3 highlights the alternative separation methods under investigation, including absorption, membrane, and adsorption based technologies [15]. Absorption based separation selectively transfers target components into an absorbent phase, leaving the remaining gases enriched. If paired with energy-efficient regeneration,

this approach could significantly reduce energy consumption compared to cryogenic distillation. Membrane separation exploits differences in component permeability across a membrane, while adsorption relies on the adherence of gas molecules to solid surfaces [15].

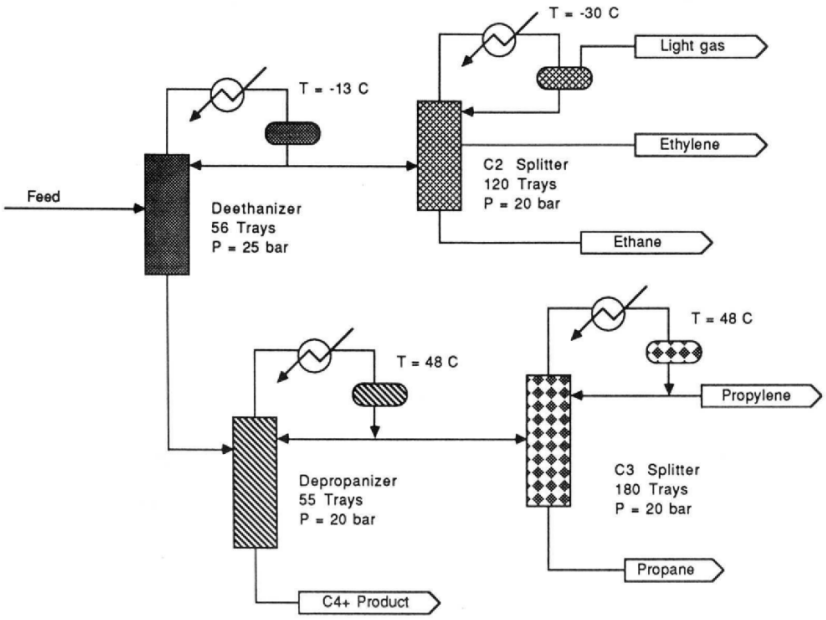

Figure 2.2: Conventional low-temperature distillation process for olefin/paraffin separation [16]

2.3 Plastic Waste

To understand the role and impact that components such as N, Cl, and S have in polymer compositions, a summary of their contributions is explained in the following paragraph.

Chlorine: normally used in polymers to improve flame-retardancy characteristics. Polymers such as PVC release HCl when heated, leading to the quenching of flames and the prevention of fire spreading [19]. Chlorine also improves chemical resistance characteristics, making them an ideal solution for its use in harsh and chemical exposure environments [19].

Sulfur: sulfur compounds are used in plastics to enhance its performance, it can be used to improve mechanical properties, thermal stability to make polymers suitable for for high temperature processes, flame-retardancy by forming a protective char layer that insulates the materials from heat, chemical resistance and adhesion, and good solubility in polar solvents because of its multiple valence states and polar character [20][21].

Nitrogen: incorporated in the backbone of polymers to enhance their stability and performance, as well as flame-retardancy by forming a char layer that that protects the material from heat and oxygen, slowing combustion [22].

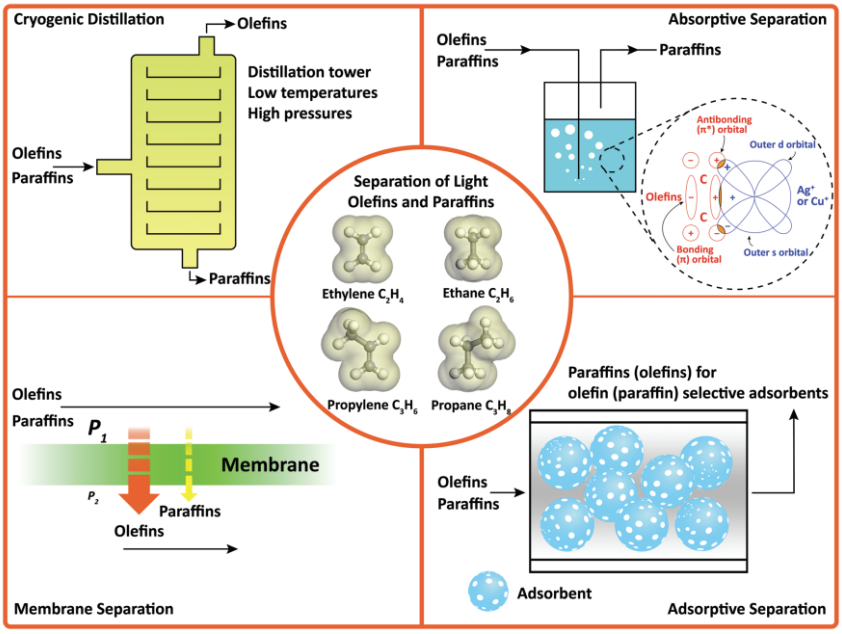

Figure 2.3: Schematic comparison of light olefin/paraffin separation processes [15]

Table A.2 and A.3 show the properties of the MPW used in this report.

2.4 Steam cracking of plastic waste

Thermochemical conversion involves a family of processes which convert feedstock into its molecular building blocks. Figure 2.4 shows three pathways for plastic waste recycling. Path A involves direct monomer recovery through thermal cracking of the feedstock, analogous to conventional naphtha/alkene cracking. However, this pathway generates non-valuable byproducts that cannot be directly reused in plastic synthesis [4]. Path B refers to the thermal decomposition of the feedstock into syngas, followed by synthesis into molecular building blocks. Path C focuses on feedstock combustion to meet heating demands while recovering carbon in the form of CO_2 [23]. To achieve complete carbon recovery, a combination of routes B and/or C with route A is necessary.

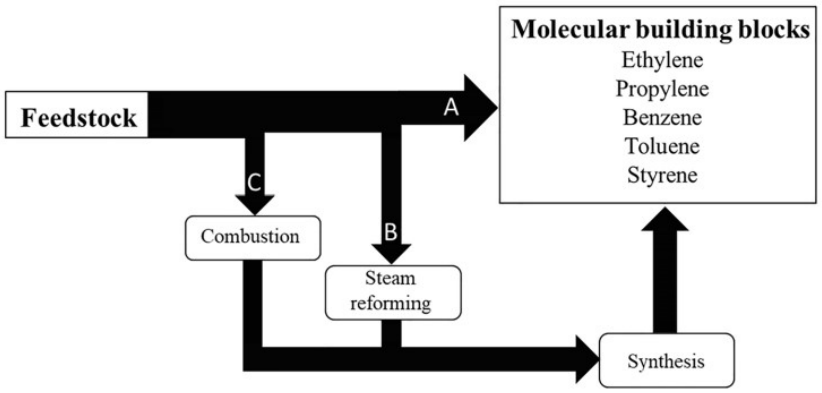

Figure 2.4: Three thermochemical recycling pathways for hydrocarbon feedstock [23].

Equation 2.1 represents the general decomposition reaction of polymer chains into shorter hydrocarbons, water, and impurities such as NH_3, HCN, H_2S, and HCl [4]. Additionally, CO, CO_2, and H_2 are generated through steam reforming and gasification [4]:

$$\mathrm{CH}_i\mathrm{O}_j\mathrm{N}_k\mathrm{S}_m\mathrm{Cl}_n \rightarrow \mathrm{CH}_\gamma + \mathrm{H_2O} + \mathrm{NH_3} + \mathrm{H_2S} + \mathrm{HCl} \tag{2.1}$$

Steam cracking of plastic waste has been demonstrated by Mandviwala et al. [10] using a dual fluidized bed (DFB) reactor as an alternative to conventional naphtha steam cracking. This process targets monomer recovery at temperatures ranging from 775°C to 825°C. The primary products from the steam cracking effluent include hydrogen, carbon monoxide, carbon dioxide, methane, ethylene, ethane, propylene, propane, butadiene, butene, isobutylene, C_5 olefins, benzene, toluene, styrene, polycyclic aromatic hydrocarbons (PAHs), and solid carbon [10]. A detailed description of the product composition can be seen in table A.4.

Figure 2.5 compares the design and operation of a conventional tubular reactor with the DFB steam cracker. In the DFB system, the circulating fluidized bed (CFB) supplies the heat required for cracking reactions. The reactor operates with natural ore bed materials, achieves short residence times, and minimizes heat transfer between the bed material and product gas above the fluidized bed, thus suppressing secondary cracking reactions [10]. A key advantage of the DFB reactor is its ability to continuously remove carbon deposits formed during steam cracking.

Compared to traditional steam crackers, the DFB reactor utilizing plastic waste generates significantly higher concentrations of carbon oxides (CO, CO_2) due to the oxygen content in plastic waste and inherent reactor chemistry, as well as a considerable amount of NH_3, HCN, H_2S, and HCl when using waste streams. Conventional processes, by contrast, produce less than 0.1% of CO_x compounds [10]. Since plastic waste steam cracking generates elevated levels of contaminants such as CO_x, H_2S,

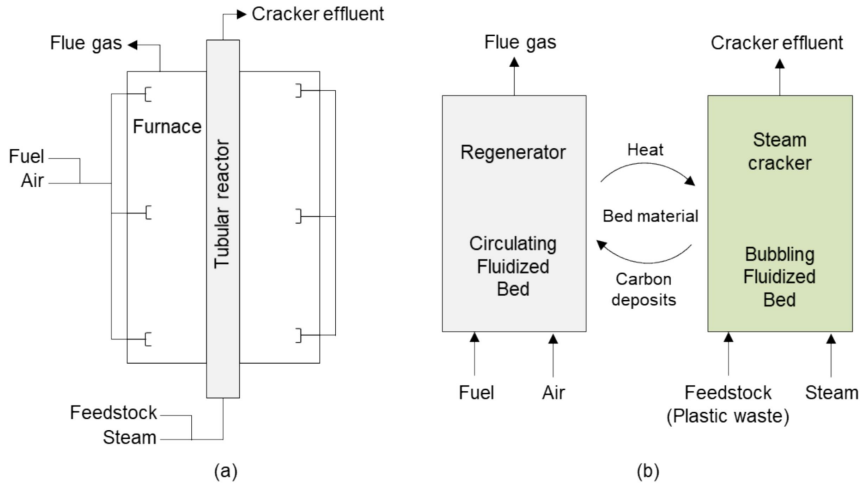

Figure 2.5: Schematic comparison of a conventional steam cracker tube (a) and a DFB steam cracker (b). Adapted from [10].

HCl, and NH_3, a gas-cleaning step is essential prior to fractionation to remove these impurities.

2.5 Water scrubbing for contaminant removal

Water has a major advantage when being used as an absorbent for gas impurities, being its availability and low cost a sufficient factor to consider its use in gas cleaning processes [11]. Water can be used in scrubbing units with a minimal concern about leakage and operating pressure. Water contact stages can also be used to quench hot gases with different purposes, such as temperature reduction, condensation of liquids, or absorption of soluble impurities. A clear example of multipurpose operation is the use of water scrubbing in coal gasification processes, where the gas is quenched and the soluble components such as NH_3 and HCl are absorbed [11]. It is important to notice that when using water absorption process to remove impurities, a minor fraction of the primary gaseous components will also be absorbed. However, this effect is noticeable at high pressures and can affect the overall balance of the process [11].

Figure 2.6 shows the counter current configuration for water scrubbing, with raw gas entering the process and going out as clean gas, while the water enters at the opposite side of the column, leaving as an acid at the bottom.

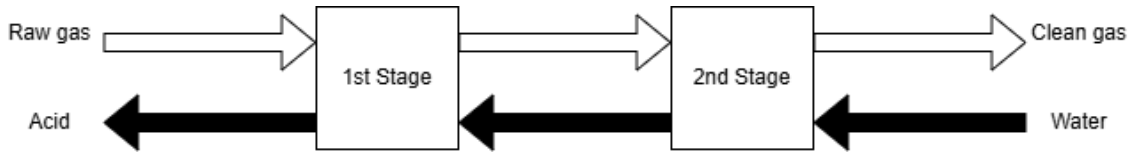

Figure 2.6: Water scrubbing diagram. Adapted from [11].

2.6 Methanol based scrubbing systems

Physical absorption involves the dissolution of gases into a liquid without chemical reactions, driven primarily by gas solubility in the liquid phase and influenced by temperature and pressure [24].

Methanol scrubbing technologies, such as the Rectisol process, are widely used in industrial gas separation. Methanol serves as an effective absorption medium due to its high solubility for target components, particularly under high-pressure and low-temperature conditions (–20°C to –70°C), which enhance selectivity [12]. However, operating at these low temperatures leads to an energy penalty due to increased refrigerant demands and power consumption [12].

The Rectisol process has gained prominence as a syngas purification technology for removing acid gases like H_2S and CO_2. The process comprises two key stages: absorption (acid gas removal) and solvent regeneration (methanol recovery). Sun and Smith [12] simulated a single and double stage Rectisol configurations using Aspen Plus, evaluating acid gas removal efficiency, heat recovery, equipment requirements, and energy consumption. These simulations provide a foundation for adapting the Rectisol process to treat steam cracking effluents from plastic waste.

Rectisol has been proven both in industrial operations and software simulations to treat sour gases efficiently, reducing the sulfur ppm to levels lower than 0.1 ppm, while also removing CO_2 [25]. It is also know for its ability to separate hydrogen cyanide, aromatics, and gum forming hydrocarbons [11].

To illustrate how methanol absorption processes are configured, an example of the Rectisol Linde technology is shown in figure 2.7. This process uses a syngas feed containing H_2S, COS, CO_2, H_2, CO, N_2, and CH_4. Syngas feed enters the bottom of the scrubbing tower T101 at -21 C, while chilled methanol enters the top at -50 C still with low viscosity, with a tower pressure of 33 bar. Due to the higher solubility of H_2S and COS compared to CO_2 in methanol, the absorber is divided into two stages, with a CO_2 rich solvent outlet, and a H_2S/CO_2 rich solvent outlet. However, as the absorption process is exothermic, an intermediate cooling stage is required to promote efficient absorption through the column [12]. Regeneration steps of the rich solvent work with flash tanks at reduced pressures to let volatile components as H_2 and CO out of the stream, as well as a flash tank D102 for CO_2 recovery. Stripping by inert gases is done in T102 to remove the remaining CO_2 in the solvent, while distillation is used both in tower T103 and T104 to separate H_2S, methanol and water respectively. Process parameters were taken from Sun et al. [12] simulation, with an operating pressure of 33 bar, a gas feed temperature of -21°C, a methanol pressure of 44 bar, and a methanol temperature of -50°C.

Solubility of hydrocarbons in physical solvents such as methanol, ethylene glycol, diethylene glycol, triethyleneglycol, and dimethyl ethers of polyethylene glycol has been compared by Nassar et al. [26]. The impact of water in the methanol scrubber solvent was also tested, for compositions between 0 to 20% weight of water.

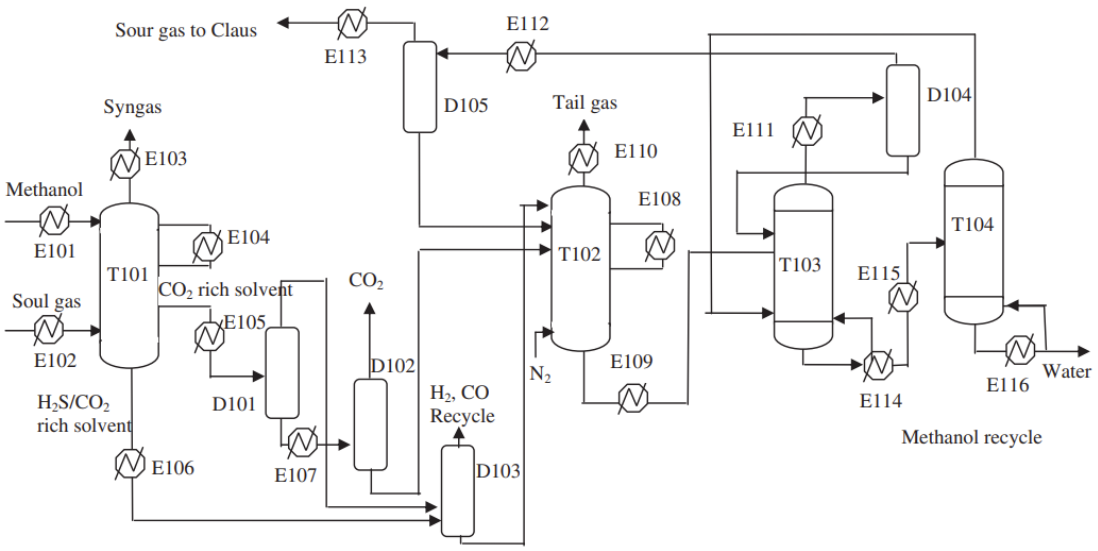

Figure 2.7: 1 Stage Rectisol Process Flow Diagram. From [12]

Increasing the water concentration leads to a decrease in the hydrocarbon pickup by 11%. However, increasing water concentration also decreases the CO_2 and H_2S absorption [26].

2.6.1 Methanol Recovery

Methanol regeneration in Rectisol processes is performed by flashing, stripping, or distillation of the methanol rich stream [12]. In flashing processes, unwanted compounds such as CO and H_2 are removed from the methanol stream (11-12 bar), to then flash and obtain a high purity CO_2 stream (5 bar) as shown in figure 2.7 unit D101 and D102. Stripping with a nitrogen stream can be used to remove any CO_2 remaining in the methanol stream after the flashing step, having a "tail gas" outlet containing N_2, CO_2, and H_2S as shown in unit T102 in figure 2.7. Distillation columns are used to separate the H_2S-methanol-water stream (T103-T104), with the sulfide going as a gas and the water-methanol stream going into a second distillation column, to dehydrate the stream (if water present in the initial gas feed). The impact of having olefins in the cold methanol stream and the separation efficiencies of contaminants that can be obtained have not been studied in previous research.

2.7 Conceptual design of the downstream cleaning process

A preliminary design of the proposed separation process is illustrated in Figure 2.8. Two models described: model 1 simulating the gasification process to obtain the energy required for the steam cracking process, while model 2 uses the cracked gas data to simulate the cleaning process.

The steam cracker effluent from the DFB reactor first undergoes cooling via two

heat exchangers configured for steam generation. This cooled stream then enters a direct contact cooler (DCC) unit for the removal of PAH, NH_3, and HCl. Next, the cracked gas stream with vapor goes through a cooling and flashing stage to eliminate the excess of water. Then, the rich hydrocarbon stream enters the methanol absorption column, which separates BTXS and remaining water, while a lighter hydrocarbon-contaminant gas stream exits the top. The methanol-rich stream goes to a distillation and regeneration unit to isolate BTXS and regenerated methanol for recycling. The removal of BTXS through compression is also simulated and compared with methanol scrubbing. Meanwhile, the light hydrocarbon-contaminant stream undergoes compression and cooling step before entering the cold methanol absorber. The outlet of this second absorption step are a methanol-hydrocarbon-rich stream, which is sent to a distillation and regeneration system for further purification, and a syngas stream with ethylene sent to the fractionation process.

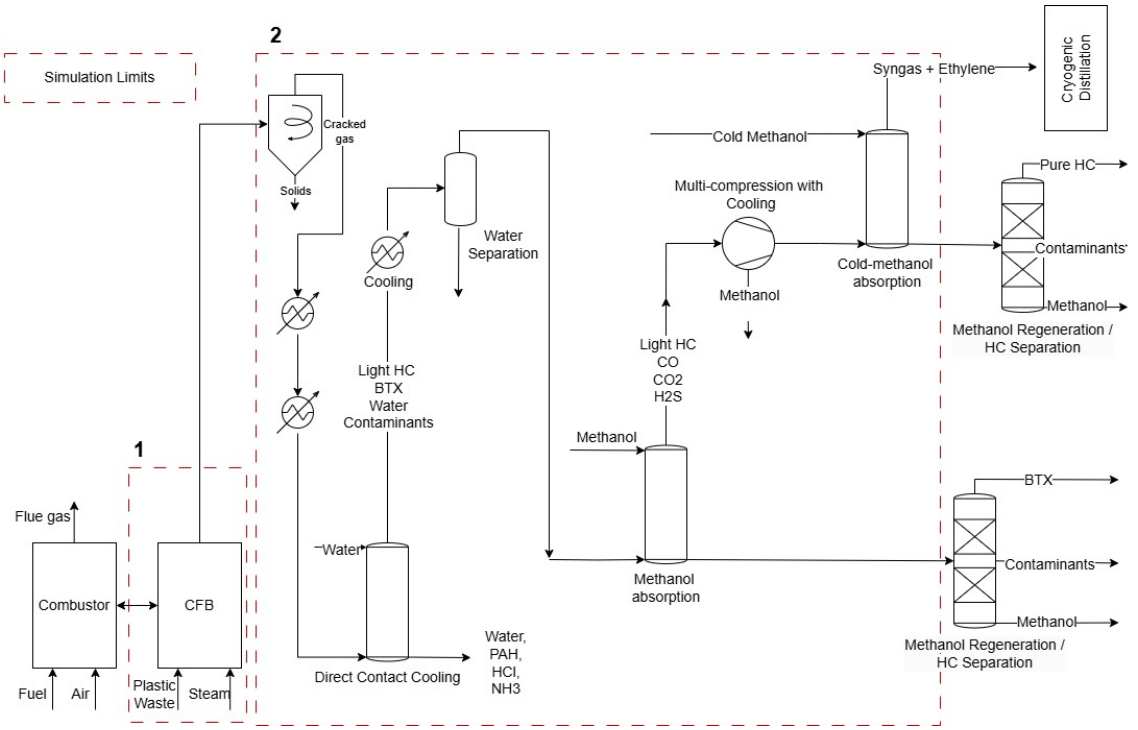

Figure 2.8: Theoretical Process Proposal.

3

Methods

This chapter focuses on describing the methodology and reasoning used during the master thesis to develop the project.

3.1 ASPEN Plus V.14

ASPEN Plus V.14. is the leading process simulator for chemical, polymer, and new sustainability processes [27]. Different thermodynamic models can be used when a simulation is run, depending on the nature of the components being analyzed. Specific models can be used when dealing with hydrocarbons, with examples being PSRK and PENG-ROB [12]. The thermodynamic models PSRK and PENG-ROB have been shown to be more accurate when simulating methanol absorption compared to RK-ASPEN and PC-SAFT[28]. The main blocks used in typical simulations are explained in the following list:

- Radfrac: used for simulating vapor-liquid equilibrium, normally used for distillation, stripping, absorption, or extractive operations. Based on MESH equations [27].
- Flash: used to simulate equilibrium based separations in a vapor and liquid phase based on the input temperature and pressure [27].
- R-Gibbs: this reactor calculates the minimum total Gibbs free energy of a system, when specifying temperature and pressure. Typical for gasification and combustion processes [27].
- R-Yield: used when no reaction mechanism or kinetics are known, but when production yields from a reaction are specified. Typically used in biomass conversion processes [27].
- Heat exchangers: conventional heating blocks are used to vary temperature instead of heat exchanger blocks (HeatX, 2 stream co-current or counter-current) to simplify the modeling process.
- Compressors: compressor blocks are used to increase the gas pressure in the system, with a typical iso-entropic efficiency of 80%, and a mechanical effi-

ciency of 98% [29].

- Pumps: pump blocks are used to increase liquid pressure in the simulation, using a typical pump efficiency of 60% and a driver efficiency of 88% [30].

3.2 Proposed Process and Modeling

Figure 3.1 shows the final diagram used for simulation in ASPEN Plus, with numbers describing the unit operations used: gasifier (1), DCC (2), flash tank (3), multi-compressor (4), and cold methanol absorber (5).

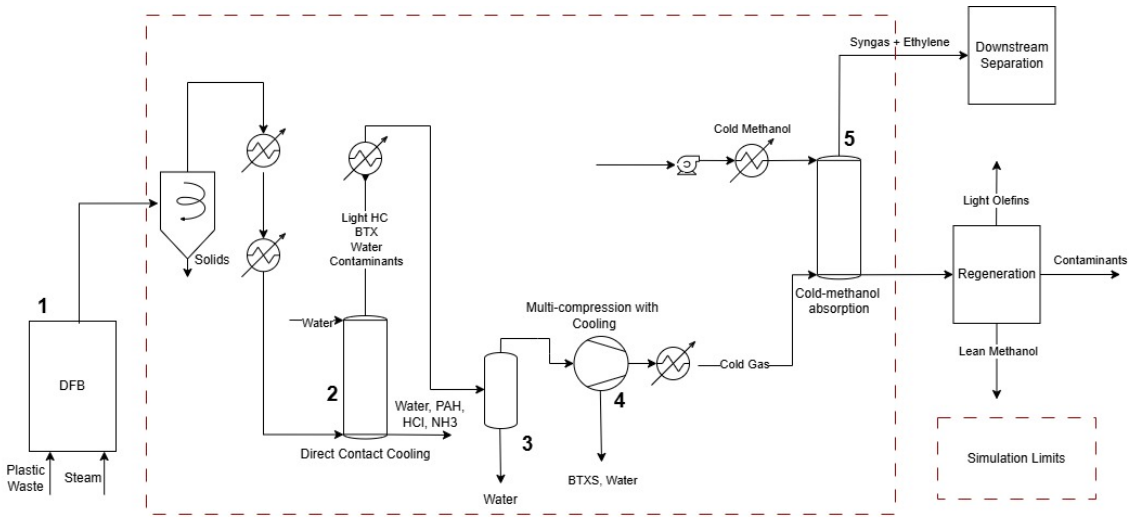

Figure 3.1: Proposed process flow diagram for simulation in ASPEN Plus.

3.2.1 Assumptions

Two different models were used during the simulation. An initial model using 1 ton/h MPW (pilot plant) to understand the feasibility of methanol absorption for the cleaning and separation of plastic waste steam cracking. Using this flowrate allows the result to be on a clear basis (per ton MPW). For sizing and techno-economic analysis presented in section 4.4 and 4.5, a second model using 12 ton/h MPW simulates an experimental plant with an expected production of 11.6 kton ethylene per year, and 5.3 ton/h PE, with the same ethylene production.

Assumptions list:

- 1 ton MPW/h for pilot plant.
- 12 ton MPW/h for experimental plant. (1608 kg/h of ethylene production)
- 5.3 ton PE/h for experimental plant. (1608 kg/h of ethylene production)
- 0.5 kg of steam / kg feed [31].

- All sulfur in the raw material is assumed to be converted into H_2S, nitrogen converted into NH_3, and chlorine converted into HCl.

Mass fractions used for the ASPEN Plus simulation can be found in table A.5.

3.2.2 DFB Steam Cracker

Figure 3.2 shows the process diagram of the Chalmers DFB reactor, represented as unit #1 in figure 3.1. It consists of a furnace (1), a cyclone for the bed recirculation (4), a particle distributor (5) which can send the particles either to the furnace (CFB mode) or to the steam cracker (6) if the process is operated in DFB mode, the bed material then returns to the furnace through the loop seal (8) [32].

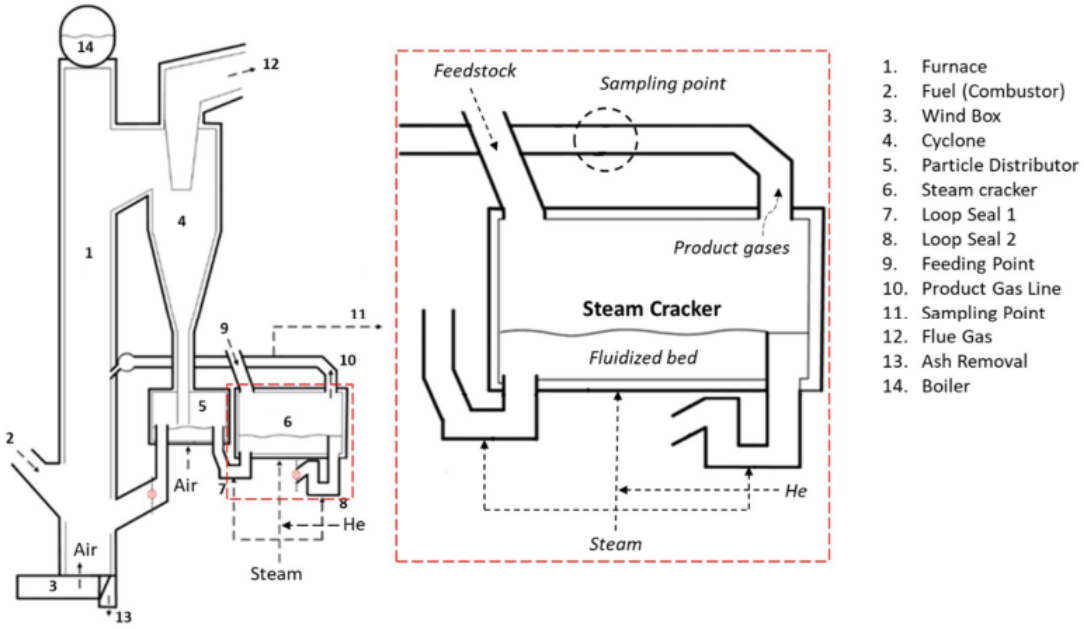

Figure 3.2: Diagram of the DFB steam cracker at Chalmers University of Technology. From [32]

Inlet data (kg product/ kg dry stock) for the ASPEN Plus model was taken from DFB steam cracking experiments [10] and adapted for its use with a 0.5 steam to plastic ratio. To understand the energy demand required for the gasification of MPW and PE, an ASPEN plus model is adapted using R-yield reactors for the decomposition of non-conventional materials (MPW and PE) into conventional ones using the elemental composition analysis shown in table A.3, and the conversion into desired product yields, shown in table A.4.

3.2.3 Solids, Acids, Water, PAH and BTXS Separation

Figure 3.3 shows the methodology followed in the separation process.

Ash and char included in the simulation are separated by using a solid separator SSplit, which only considers the specified fractions going as a fluid and as a solid.

Next, it is relevant to understand the impact of temperature and pressure in the condensation of water, PAH, BTXS, and contaminants by using a heat exchanger and flash system. The main outcome of this simulation will be different condensation efficiencies at different process parameters.

After this, a first methanol absorber test using a RadFrac unit is done, to understand the impact and absorption efficiency of the process while manipulating pressure and temperature, targeting the removal of aromatic compounds on the cracked stream. From this step, methanol flowrates required for absorption at different conditions are obtained.

HCl and NH_3 water scrubbing (DCC) is then simulated with a RadFrac block using reference data [33] for the removal of unwanted materials from off gases, while PAH condensation is also evaluated by using a water scrubbing system, simulated with a RadFrac block. The main takeaway from this step is the water flowrate required to quench the gas, condense PAH, and absorb HCl and NH_3, as well as the removal efficiency for these components.

A condensation step is added with a concenser block and a flash block to eliminate excess water before entering the methanol scrubber, to reduce the methanol consumption and understand the benefits of adding this separation step. A sensitivity analysis using different temperatures is performed to select an adequate flashing temperature.

A second methanol absorber test using a RadFrac unit is done, to understand the impact and absorption efficiency of the process while manipulating pressure and temperature without the water excess on the stream. From this step, new methanol flowrates required for absorption at different conditions are obtained, as well as the ideal operating pressure and temperature.

Ratio equation 3.1 and 3.2 describe the amount of methanol needed to absorb benzene and BTXS respectively.

$$\text{Benzene Ratio} = \frac{\text{Methanol (kg/h)}}{\text{Absorbed Benzene (kg/h)}} \tag{3.1}$$

$$\text{BTXS} = \frac{\text{Methanol (kg/h)}}{\text{Sum of Absorbed BTXS (kg/h)}} \tag{3.2}$$

Finally, an analysis of the feasibility of implementing methanol absorption for BTXS removal is done, as well as a discussion about the regeneration challenges of methanol after the absorption process. ASPEN Plus azeotrope search tool is used to identify the azeotropes present when having a methanol-water-hydrocarbon mixture.

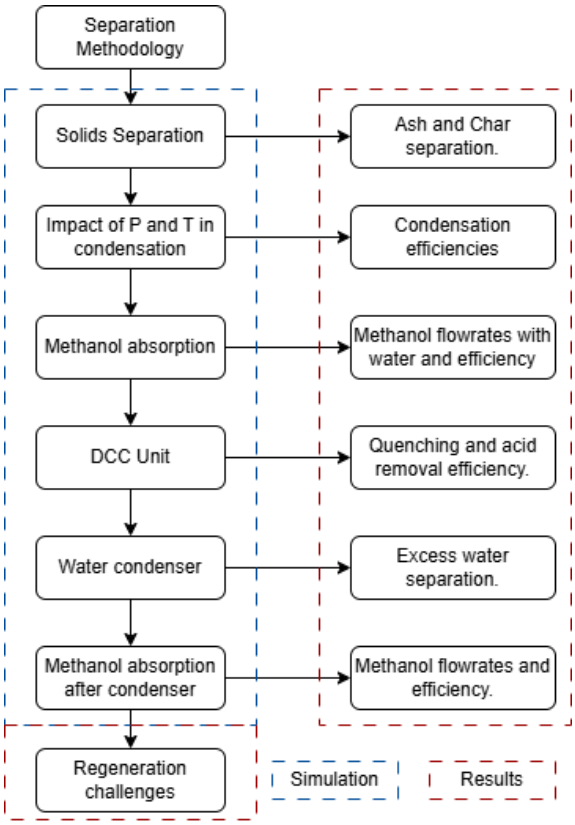

Figure 3.3: Separation process methodology.

3.2.4 Compression steps

As typical Rectisol technologies for acid gas treatment require high pressures, ranging from 33 bar to 50 bar [12] a compression step is needed to reach the absorber inlet conditions. A multi stage compressor can be used to meet this requirement, with some of the advantages being less power required compared to a single stage compressor, higher volumetric efficiency, and cheaper materials due to the inter cooling stages. Some of the disadvantages when dealing with a multi stage compressor are the increase in the initial cost, complexity on the inter cooling stages, pressure losses, and complex construction [34]. The work of Arvidsson et al. [35] shows a multi compression step used to increase a gasified stream up to 40 bar, while using an inter cooling temperature of 40 °C, while obtaining a knock stream, as presented in figure 3.1.

3.2.5 Rectisol Technology - Cold methanol absorption

A cold methanol absorption process following process parameters of the Rectisol technology is evaluated, and shown in the process diagram of figure 3.4. An inlet pressure of 33 bar for the gas is used, with a temperature of -21 °C. A methanol pressure of 44 bar is used, with an inlet temperature of -50 °C. A sensitivity analysis measuring the impact of methanol flowrate and operating pressure is performed to find the best process parameters for light olefins absorption and contaminant removal (CO_2 and H_2S). Different flash pressures in the CO_2 flashing step are also

studied to identify the CO_2-ethylene mix going out as a gas in this first separation step. An analysis of the expected challenges presented when regenerating methanol rich in olefins, CO_2, and H_2S is described in the results section.

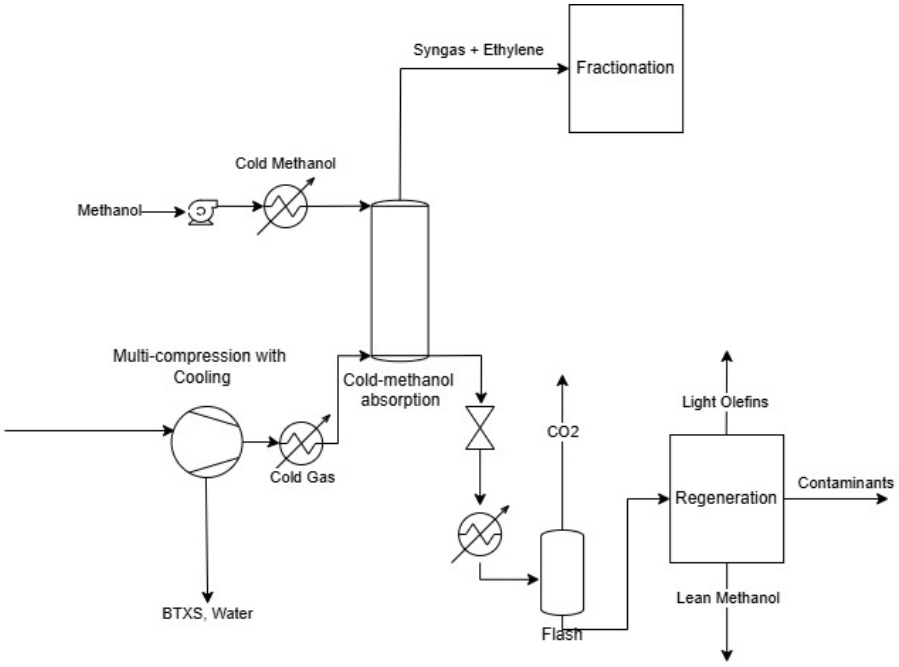

Figure 3.4: Cold methanol absorption process diagram.

3.2.6 Utilities

Different utilities are needed for the process. Utilities and assumptions considered are described in the following section.

Cooling water: varying between 5 and 15 °C depending on the time of the year, selecting an average of 10 °C.

Refrigeration: cooling temperatures of -60°C for cold methanol and -40°C cracked gas cooling are needed. Propylene can be used for refrigeration medium.

Electricity: costs are assumed from NordPool data in area SE3 [36], with 2025 price being 600 SEK/MWh.

3.3 Equipment Sizing

ASPEN Plus sizing tools are used to obtain major equipment dimensions. Wall thickness was calculated using equation 3.3 [37] to later calculate the shell mass, where SE represents the maximum stress, Di the internal diameter, and Pi the internal pressure. To calculate the total shell mass for its use in the CAPEX equations, equation 3.4 [37] was used, where D_c represents the vessel diameter, L_c the vessel length, t_w the wall thickness, and ρ the metal density.

$$t = \frac{P_i D_i}{2SE - 1.2P_i} \tag{3.3}$$

$$\text{Shell mass} = \pi D_c L_c t_w \rho \tag{3.4}$$

3.3.1 Direct Contact Cooler

The direct contact cooler was sized in ASPEN Plus, with the material selected being stainless steel 304 to resist corrosion from chlorides and ammonia. 2 mm of additional wall thickness are estimated to prevent corrosion [37]. The diameter for the column is obtained from the ASPEN Plus simulation.

3.3.2 Flash Tank

The flash tank size is determined by using ASPEN Plus stream properties, such as liquid and gas density before entering the condensation unit. Equation 3.5 is used to determine the settling velocity in the flash tank, while equation 3.6 is used to calculate the vessel diameter. The use of a mist eliminator (demister pad) can be considered to avoid any liquid carryover in the gaseous stream.

$$u_t = 0.07\sqrt{\frac{\rho_L - \rho_v}{\rho_v}} \tag{3.5}$$

$$D = \sqrt{\frac{4Q}{\pi u_s}} \tag{3.6}$$

3.3.3 Cold Methanol Absorber

The cold methanol absorber was simulated in ASPEN Plus using different methanol flowrates and total number of stages, with the design parameter being 0.5 ppm of CO_2 in the ethylene rich syngas stream, as mentioned by Zimmerman [38] regarding CO_2 concentrations for ethylene production. Diameter size and number of stages were calculated from the simulation results.

3.4 Techno-economic Analysis

Estimating purchased equipment cost with chapter 3 of Chemical Engineering Design [37]. The main assumptions for the techno-economic analysis are shown in table 3.1.

3.4.1 CAPEX

Table 3.2 shows the different factors used for the capital cost estimation, obtained from [37]. Equation 3.7 and 3.8 are used for the CAPEX estimation.

Parameter	**Value**
Economic lifetime of the plant	20 years
Interest rate	5%
Annual operating time	8000 h/year
Working capital	5% of fixed capital
Ethylene Market Price	\$810 USD/ton
Propylene Market Price	\$830 USD/ton
Benzene Market Price	\$690 USD/ton
Toluene Market Price	\$800 USD/ton
Styrene Market Price	\$860 USD/ton

Table 3.1: Main assumptions for the techno-economic analysis

Unit Operation	Measure	Equation	Cost Unit
Pressure Vessel (CS)	Shell mass (kg)	$11600 + 34S^{0.85}$	USD (2010)
Pressure Vessel (SS)	Shell mass (kg)	$17400 + 79S^{0.85}$	USD (2010)
HEX	m^2	$28000 + 54S^{1.2}$	USD (2010)
Trays	#	$130 + 440S^{1.8}$	USD (2010)
Pumps	kW	$8000 + 240S^{0.90}$	USD (2010)
Compressor	kW	$240000 + 1.33S^{1.5}$	USD (2010)
Tanks (floating roof)	m^3	$113000 + 3250S^{0.8}$	USD (2010)

Table 3.2: Capitacl cost estimation factors. Adapted from [37].

$$C_e = a + b\,S^n \tag{3.7}$$

$$CC_{\text{year 2024}} = CC_{\text{year } x} \cdot \frac{CEPCI_{\text{year 2024}}}{CEPCI_{\text{year } x}} \tag{3.8}$$

The CEPCI Index for June 2024 is 798.8 [39], and will be used for the capital cost calculations. CEPCI cost for 2010 will be assumed to be 550.8 [39]. Table 3.3 shows the typical fixed capital cost factors for fluid-solid processes [37]. Working capital will be assumed to be 5% of the fixed capital cost.

Table 3.3 is used to transform the calculated equipment cost into fixed capital cost, considering a plant dealing with fluids and solids.

Item	Fluids–Solids (C_i)
f_{er} Equipment erection	0,5
f_p Piping	0,6
f_i Instrumentation and control	0,3
f_e Electrical	0,3
f_c Civil	0,3
f_s Structures and buildings	0,2
f_l Lagging and paint	0,1
ISBL cost, $C = 1 + \Sigma C_i$	3,2
Offsites	0,4
Design and Engineering (D&E)	0,25
Contingency	0,1
Total fixed capital cost	**3,95**

Table 3.3: Fixed capital cost factors for fluids–solids processes. From [37].

The gasification island CAPEX, including the fuel handling system, gasification and combustion, and flue gas system [40] will be estimated by using equation 3.9 and the factors and costs described by Thunman et al. [41] in the economic analysis of biofuel production via gasification, where $C_{\text{inv},i}$ refers to the investment cost, $C_{\text{inv},ref,i}$ refers to the reference investment cost, P refers to the desired capacity, P_{ref} refers to the reference capacity, and SF refers to the conversion factors.

$$C_{\text{inv},i} = C_{\text{Inv,ref},i} \left(\frac{P}{P_{\text{ref}}} \right)^{\text{SF}_i} \tag{3.9}$$

	System	Ref. cost (kSEK)	SF low	SF	SF high
1	Fuel handling system	50,400			
1.1	External fuel feeding system		0.50	0.60	0.70
1.2	Internal fuel feeding system		0.40	0.50	0.60
2	Gasification and Combustion	29,490			
2.1	Reactors and refractory		0.60	0.70	0.80
2.2	Condensate treatment		0.50	0.60	0.70
3	Flue gas system	18,930			
3.1	Flue gas cooler		0.70	0.80	0.90
3.2	Flue gas filter and fan		0.70	0.80	0.90
3.3	Ash handling system		0.60	0.70	0.80

Table 3.4: Investment cost and scale factors for gasification island. Adapted from [41]

An annuity factor is used to evaluate the annual capital cost, following equations

3.10 and 3.11, where n stands for the expected lifetime of the plant, and i for the interest rate.

$$\mathrm{ACC} = \mathrm{FCC} \cdot a \tag{3.10}$$

$$a = \frac{i}{1 - (1+i)^{-n}} \tag{3.11}$$

3.4.2 OPEX

The OPEX will be divided in two different sections: the variable operating costs, including raw materials and utilities, and fixed operation costs, including maintenance, labor supervision, management, rate on capital, insurance, taxes, and R&D. Recommended assumptions for fixed operational costs, such as maintenance, labor costs, laboratory, insurance, and taxes will be used [37].

Refrigeration costs are determined by using equation 3.12 [42], considering a temperature of -60 °C for the cryogenic refrigeration temperature.

$$\mathrm{Cost}(\$/\mathrm{kWh}) = \frac{\exp\left(2.4647 - 0.01812T(^{\circ}\mathrm{C})\right)}{277.78} \tag{3.12}$$

Raw materials and utilities used for the calculation of variable operation costs are shown in table 3.5.

Raw materials and utilities	Price	Unit	Year	Reference
MPW Medium Term	0	USD/ton	2013	[4]
Methanol	660	USD/ton	2013	[43]
Electricity	60	USD/kWh	2025	[36]
Refrigeration	0.13	USD/kWh	2017	[42]
Steam	0.03	USD/kWh	2017	[42]
Wood Chips	25	USD/MWh	2023	[44]

Table 3.5: Raw materials and utilities costs.

3.4.3 Sensitivity Analysis

The impact of the calculated CAPEX and OPEX will be studied for PE and MPW, calculating the production cost for ethylene, propylene, and benzene in different scenarios, such as a decrease of 20% in the CAPEX and OPEX, increase of 50% in the CAPEX and OPEX, and the combination between them. Increase in CAPEX is used to simulate the additional equipment needed to complete the separation and cleaning process, such as the distillation columns and flash tanks in the cold

methanol absorption process. The increase in the OPEX will simulate fluctuations in the refrigeration, fuel, steam, and electricity prices.

4

Results and discussion

This chapter summarizes the main results of the ASPEN Plus simulation when using the assumptions and technologies described in chapter 3. Results include the primary fractionation process for the removal of PAH and contaminants, DCC, methanol absorption of BTXS, cold methanol absorption of light olefins and contaminants, equipment sizing, techno-economic analysis, and sensitivity analysis of the overall process.

4.1 Primary fractionation (Water, PAH, BTX and contaminant separation)

As shown in table A.4, the different raw materials used for the steam cracking process have a product composition containing PAH's, BTX, contaminants, and water coming from steam and moisture. The impact of temperature and pressure in the condensation of the specified components was analyzed, as well as the performance of water scrubbing (DCC), water condensation through a flash tank, and methanol absorption. This section is divided in three different subsections: temperature and pressure effect, water DCC, and methanol absorption.

4.1.1 Water DCC

Figure 3.1 show the DCC as process #2, where HCl and NH_3 scrubbing was simulated using equilibrium reactions published by Ganeth et al. [33] According to Kohl [11] typical water scrubbing towers for ammonia removal lead to a change in concentration from 200-500 g/scf to 2-7 g/scf. The mole fraction equivalent is 0.06-0.15 to 0.0006-0.002. A caustic stripping process could be used if ammonia recovery is desired. The initial values for ammonia and HCl in the MPW cracked stream are shown in table A.5, being 0.5% wt. HCl and 0.4% wt. NH_3. Figure 4.1 shows the fraction of feed going at the gas outlet of the DCC vs different water flow rates. As shown in the figure, increasing water flowrate increases the PAH removal from the gas stream, while maintaining HCl and NH_3 values constant. Aromatics and olefin compounds do not interact with water and go out as gas.

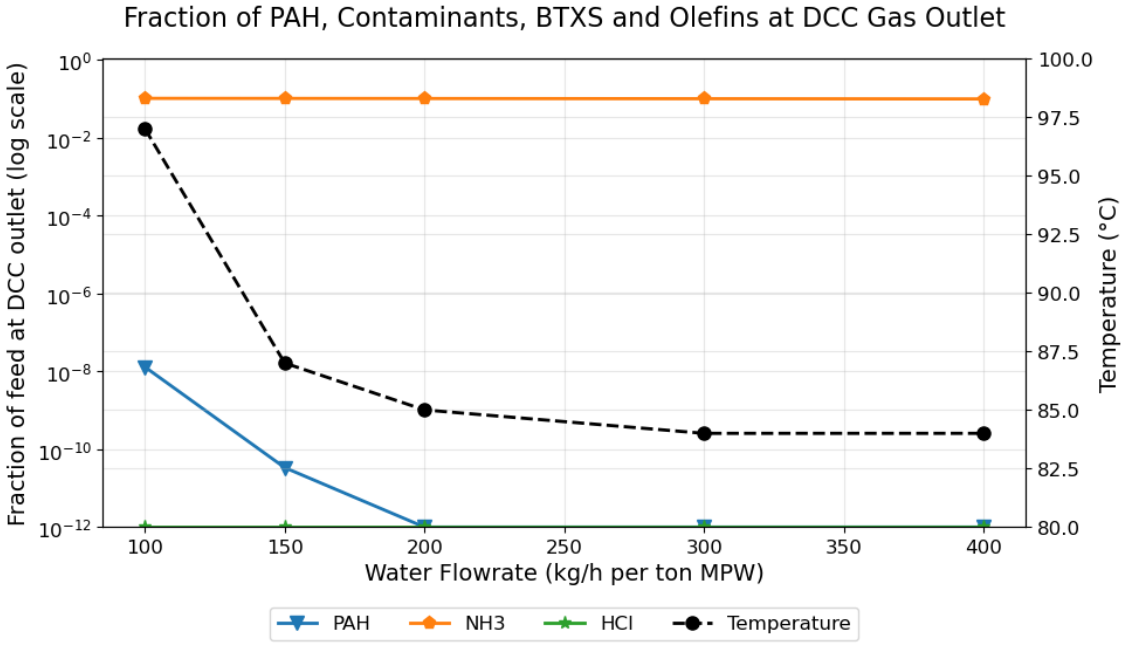

Figure 4.1: Fraction of feed going out as gas in the DCC Unit.

A flow rate of 200 kg/h of water per ton MPW in the DCC was selected to remove the PAH and HCl fractions completely, while reducing the NH3 mole fraction from 0.006 to 0.0005. Selecting a higher flowrate will not affect the PAH removal considerably, while selecting a lower one will reduce PAH removal. PAH is totally condensed, while BTXS fractions and light olefins leave the DCC unit as a gas to enter the next process stages. Diameter and stages are obtained from the ASPEN Plus simulation.

4.1.2 Effect of pressure and temperature

The impact of adding a cooler and flash tank to condensate water, PAH, and contaminants instead of the DCC unit was also studied as an alternative for process # 2. Figure 4.2 shows the effect of varying pressure and temperature to the cracker effluent coming from the steam cracking process. Temperature ranges from 50 to 200 °C and pressures from 1 to 10 bar were used in Aspen Plus to understand the impact they have in a first condensation step. Removal fraction (0 to 1) are shown in the Y axis, while temperature is shown in the X axis, and the different line colors represent different operating pressure.

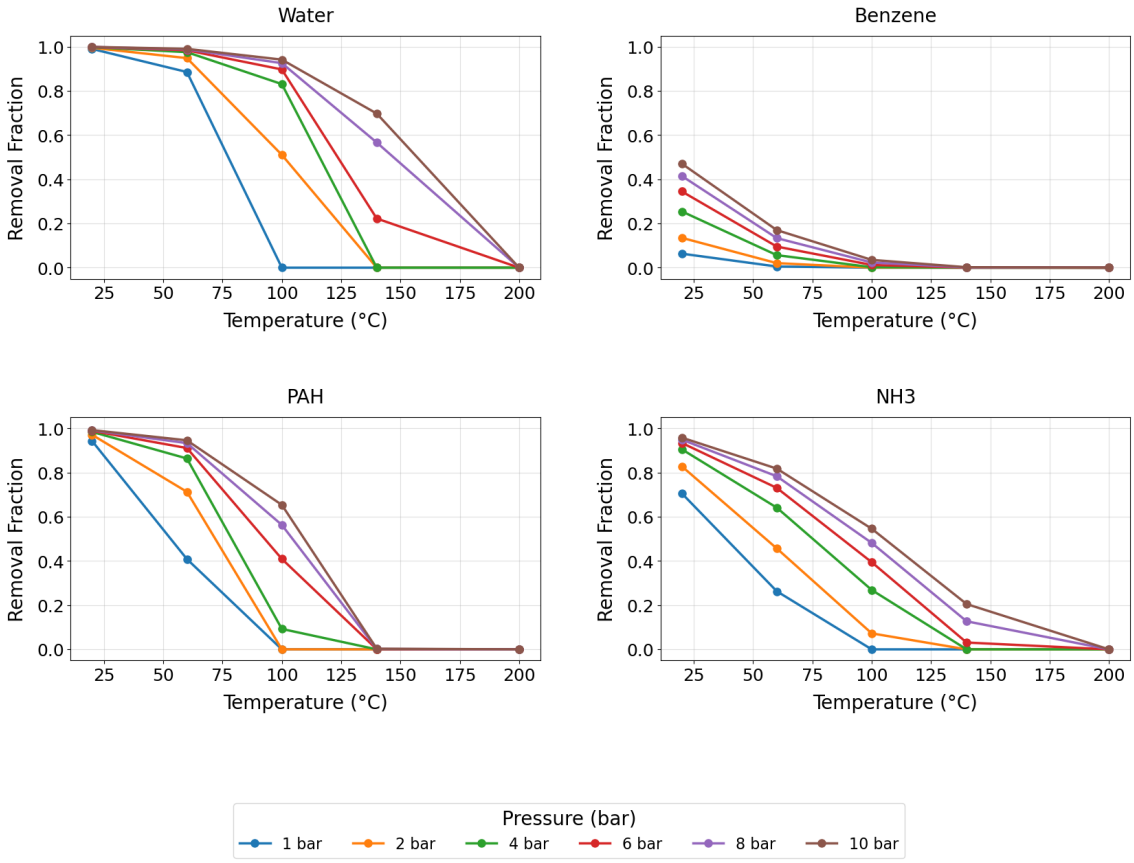

Figure 4.2: Removed fraction of components vs temperature at different pressures.

It can be seen that 90% of the water can be removed at 1 bar when reaching a temperature of 50 °C. BTXS condensation is less than 5% of total BTXS weight at the same conditions. 60% of the PAH feed is also condensed at this conditions, while NH_3 is condensed in approximately 60%. A pressure increase is required to totally remove PAH and NH_3 in this step. For H_2S and HCl, there is no relevant removal in this condensation step. The impact of pressure leads to a higher temperature when achieving similar removal efficiencies for the components. A pressure of 8 bar at 50°C is needed to condensate excess water and PAH, without removing HCl and NH_3 completely. Due to these results, the DCC unit (#2) is a better option for PAH and acid removal (HCl and NH_3).

4.1.3 Methanol Absorption for BTX removal and regeneration

The cracked gas stream coming out from the DCC was used to evaluate the performance and feasibility of a methanol absorption system for BTXS removal without a condensation step to remove water excess. The absorption simulation was done in ASPEN Plus using a RadFrac column with equilibrium calculations, with methanol entering the top of the column at 20°C and 1 bar, while the gas inlet enters at the bottom.

Figure 4.3 shows the fraction of BTXS and water going out as a gas in the methanol absorber in the Y axis. It can be seen that increasing the methanol flowrate in the X axis leads to better removal of BTXS. Pressure also impacts the methanol absorption, as higher pressures lead to a lower methanol demand while removing the same fractions. In this case, at least a flowrate of 3000 kg/h methanol per ton MPW is needed to remove benzene below the 1% threshold. Results lead to the implementation of a water condenser before the absorption step.

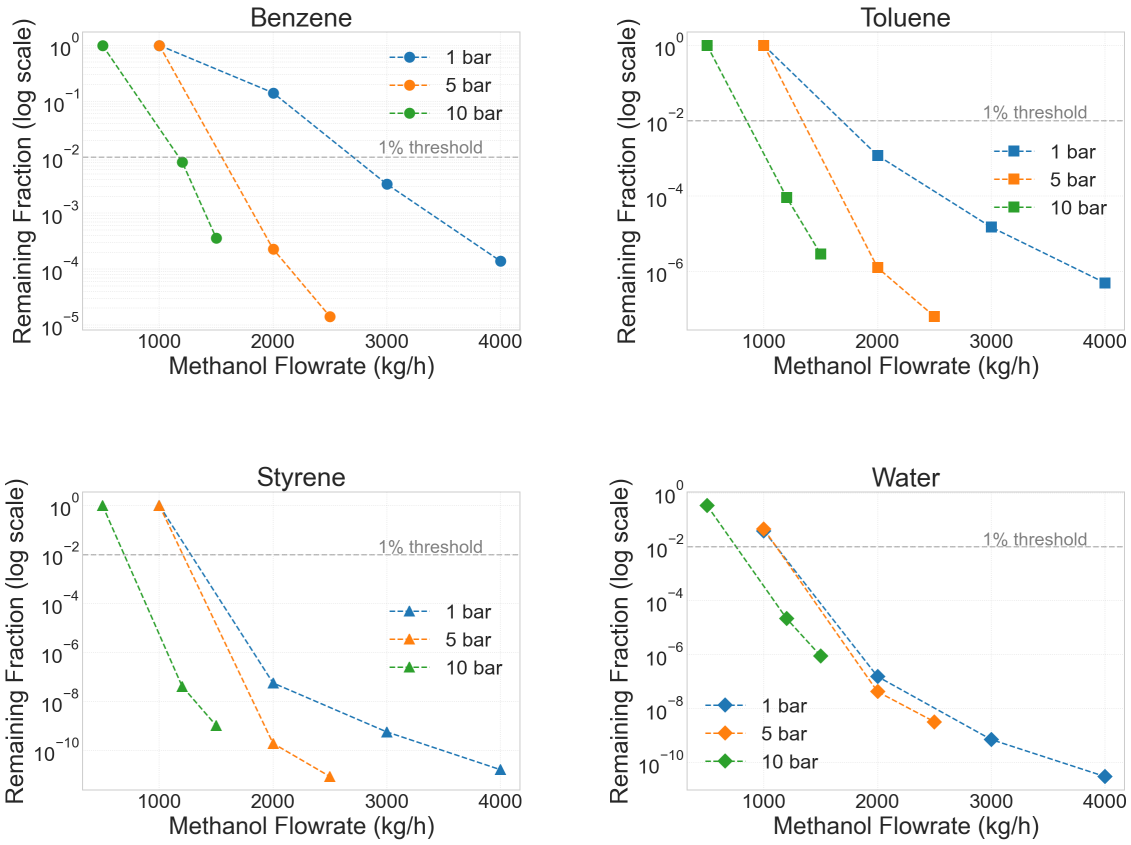

Figure 4.3: Methanol flowrate required to remove water and BTXS at different pressures per ton MPW.

4.1.3.1 Water condenser

A condensation step was included in the simulation to reduce the mole fraction of water entering the methanol absorber (unit operation # 3 in figure 3.1). A sensitivity analysis was performed by varying the cracked gas temperature with a heat exchanger, followed by a flash stage were the water fraction is condensed. The sensitivity analysis results show that decreasing the temperature will lead to a higher fraction of water removal, however this low temperatures could also lead to hydrocarbon condensation. To avoid hydrocarbon condensation, a temperature of 50 °C was selected for the flash step, with 99.9% of the condensed stream being water. The sensitivity analysis done for the flash tank is shown in figure B.3.

4.1.3.2 Methanol absorption after flash condenser

The impact of methanol temperature (-40 °C to 20 °C) and absorption pressure (1 bar to 10 bar) was also analyzed in the simulation, with the main results presented in figures 4.4 and 4.5. Colder temperatures lead to an increase on the absorption of BTXS, as figure 4.4 shows. At 1 bar and 300 kg/h methanol per ton MPW, there is a difference of 10% in the removal efficiency for BTXS when comparing the coldest and warmest streams. However, when increasing flow rates to obtain higher absorption rates (700 kg/h) this absorption difference between temperatures decreases, being just 0.5% difference between the -40 °C and 20 °C methanol streams. Cold methanol temperatures are normally used in absorption processes to avoid methanol losses going with the gaseous stream. Using cold methanol in a temperature of -40 °C will result in a high refrigeration demand, needing approximately 86 kW per ton MPW to cool down the methanol stream from 20 to -40 °C.

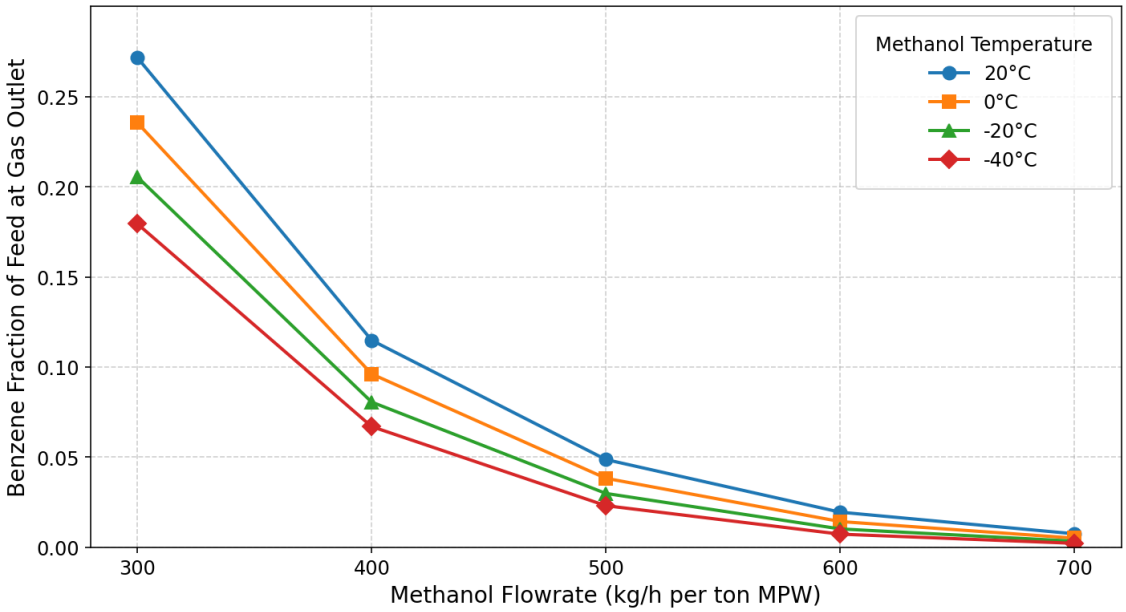

Figure 4.4: Fraction of feed going out as gas in the Methanol Absorption Unit at 1 bar.

The use of different absorption pressures have a bigger impact on absorption efficiency. The following operating pressures were analyzed in the simulation, being 1, 5, and 10 bar. Figure 4.5 shows the ratio of methanol flow rate per ton of MPW to absorb 99% of the benzene fraction in the initial feed. Ratio equation 3.1 and 3.2 describe how the ratios for both graphs in figure 4.5 were calculated.

Pressure plays a big role in the methanol absorption of BTXS. The increase the operating pressure from 1 bar to 10 bar leads to a decrease in the methanol mass required to reach 1% benzene in the gas stream. 12% of the methanol flowrate at 1 bar is needed to achieve the same removal at 10 bar, while 22% is required to operate at 5 bar. Pressurizing will also lead to the investment of a compression system and high pressure vessels, as well as the operational cost for electricity.

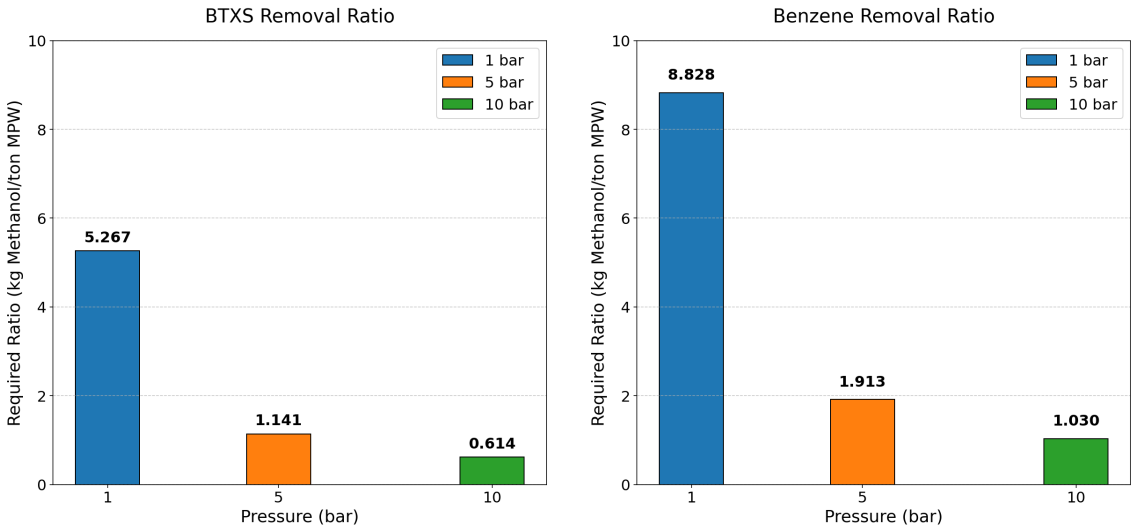

Figure 4.5: Ratio of methanol @20°C to MPW to remove BTXS fractions to less than 1% of initial benzene fraction.

4.1.4 Regeneration Challenges BTXS

Methanol rich streams need a regeneration process for the solvent to be recycled within the process. ASPEN Plus azeotrope search tool was used to understand the behavior of the obtained mixture after the methanol-BTXS absorber, and details can be found in Appendix C. 7 relevant azeotropes were found at 1 bar, with benzene-methanol, benzene-methanol-water, and benzene-water being the most relevant because of the high compositions they have in the rich methanol stream. This azeotrope formation will lead to a separation limit for methanol regeneration, as methanol-water compositions require high energy demands to be fully separated. The similar volatilities of BTXS components will also lead to an intensive separation.

Multi-stage separation will be needed to purify the methanol streams for its reuse in the process, making this option less attractive in terms of efficiency. As a multi-compressor system is required for the downstream process, the feasibility of removing BTXS from this step is analyzed in section 4.2.1.

4.2 Cold Methanol Use for Ethylene Separation

A RadFrac absorption column in equilibrium mode was used to simulate the cold methanol absorption process. The system consists of a methanol stream at 20 °C that then goes through compression (44 bar) and cooling (-50 °C) stages before entering the absorption column. The gas streams enters the absorption system at 33 bar, increasing the pressure from 1 to 33 bar in a multi stage compression with 40 °C inter cooling, having an outlet gas stream and a knock out liquid stream. After absorption, a regeneration step needs to be implemented to recover methanol for its recycling, as well as to obtain separated CO_2, H_2S, and olefin streams.

This section is divided into 3 different subsections: compression and cooling, cold methanol absorption, and regeneration challenges.

4.2.1 Compression and cooling

Figure 4.6 shows the removal of the main organic components in the stream entering the multi-stage compression system. 90% of the total benzene is removed in the multi-stage compressor, while 99% of toluene and styrene is recovered. Water is also removed from the gas stream, with 97% being condensed. Light olefins present in the stream also condense, removing 44% of total pentane, 20% of butadiene, 6% of propylene, and 1% of ethylene. The removal of these light olefins reduce the overall product yield, and therefore lowers the total profitability. It will also have an impact in the aromatics separation process.

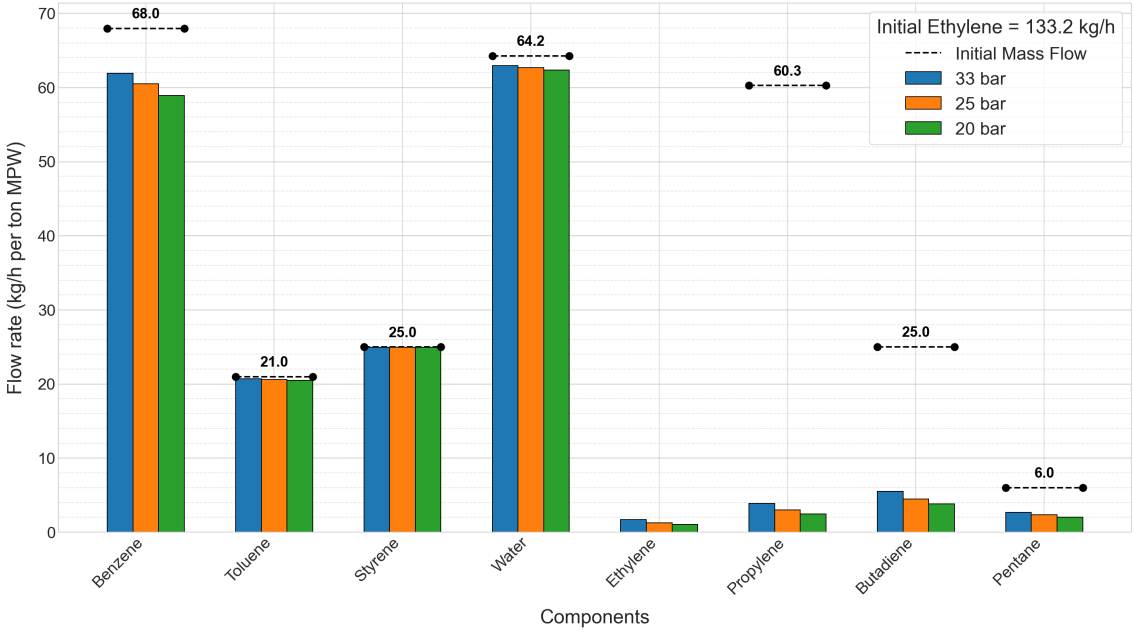

Figure 4.6: Knock out flowrates at different compression outlet pressures.

90 % of benzene and all remaining aromatics are recovered with the multi-stage compression system that is required for the cold methanol absorber downstrean in the process. Even though light olefins are condensed in this step, it avoids a methanol feedstock and energy intensive regeneration process as methanol absorption will require. Comparing the BTXS-methanol absorption process with the multistage compression, the multi-stage compression with BTXS recovery as knockout liquid is the best option to use in the process, and is included in figure 3.1 as process # 4. The total energy requirements for compression and cooling in the multi-stage compression is specified in section 4.4 and 4.5.

4.2.2 Cold methanol Absorption

The cold methanol simulation was performed in ASPEN Plus with an absorber pressure of 33 bar, a gas stream at -21 °C, and a cold methanol stream at -44°C for

an initial MPW flowrate of 1 ton/h. Figure 4.7 shows the impact of methanol flow rate in the gas going out of the absorber (syngas) concentration. It can be seen that when decreasing the methanol flowrate, CO_2 and ethylene absorption decreases, while when rising methanol flowrate absorption of both CO_2 and ethylene fractions increase. For the syngas fraction, the increase of methanol only affects methane absorption, which can be desorbed in the regeneration process. Figure 4.8 shows the fraction of the components being absorbed in the cold methanol stream, showing that for removing +90% of ethylene a flowrate of more than 3000 kg/h methanol is needed. High methanol flowrates will be needed to absorb all ethylene present, making the separation process more intensive in terms of energy and equipment size. The process could be designed by minimizing the methanol use, while absorbing the required amount of CO_2. Using this approach, syngas-ethylene rich stream will go out as gas from the cold methanol absorber and sent into a typical cryogenic distillation process as shown in figure 3.1 unit # 5, while the methanol rich stream will go through a regeneration stage, where CO_2 and H_2S must be separated, as well as the remaining ethylene, propylene, butadiene, and other hydrocarbons present in the stream.

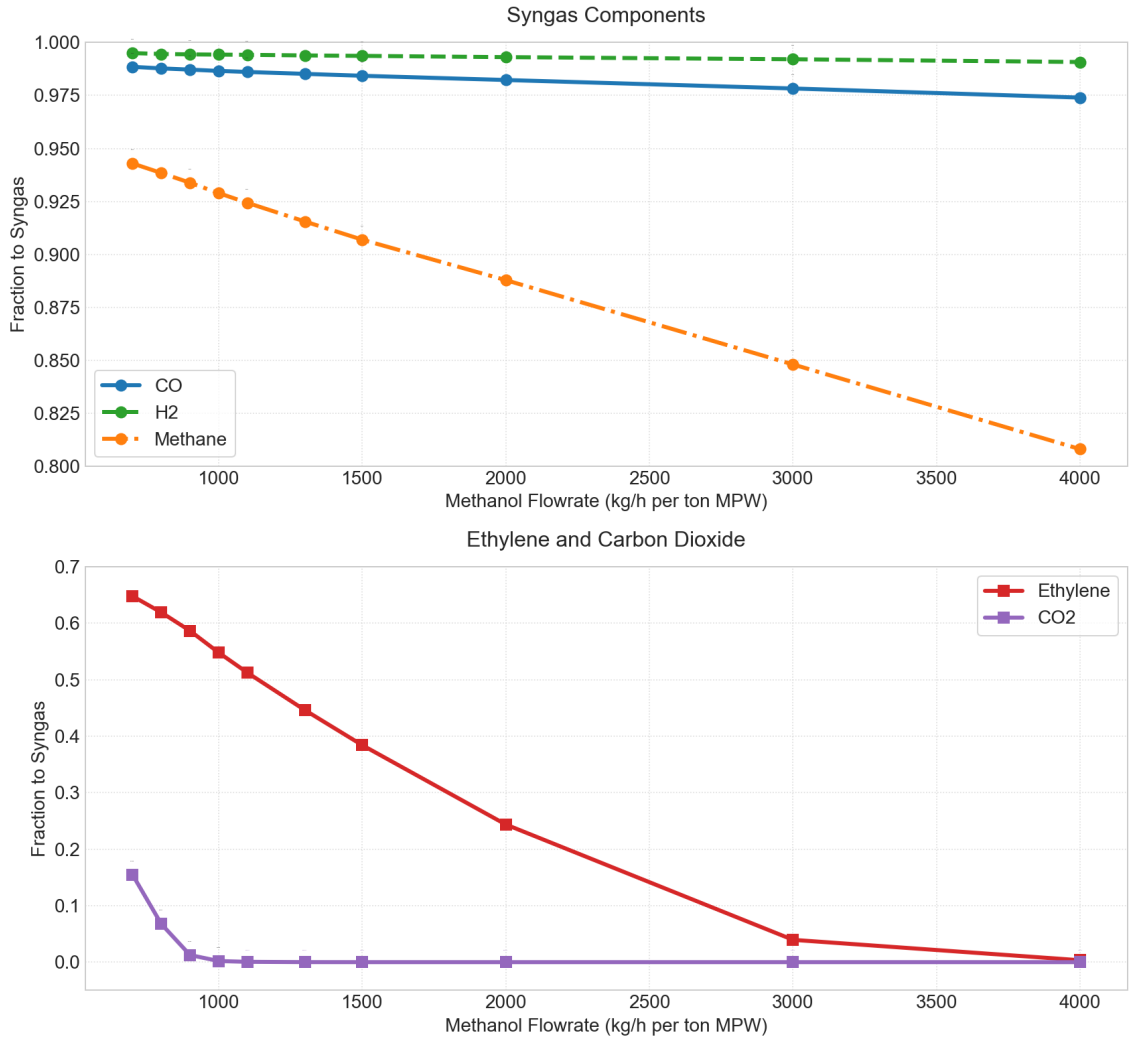

Figure 4.7: Fractions of light gases recovered in the cold methanol absorber.

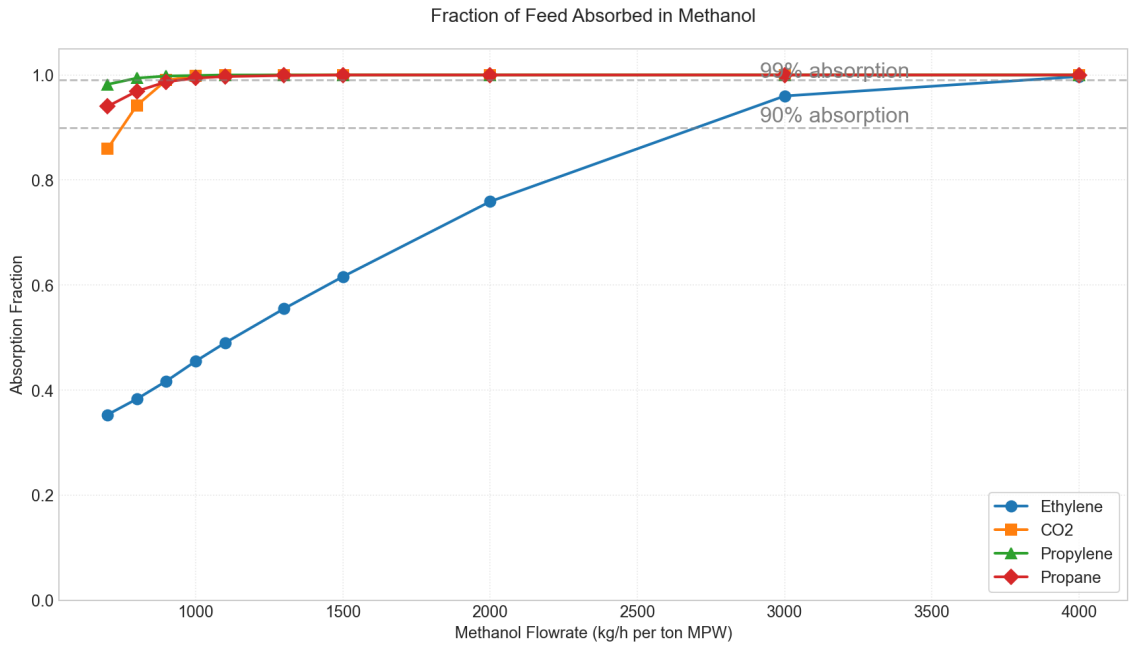

Figure 4.8: Fractions of components recovered in the cold rich methanol liquid stream.H_2S and butadiene are fully absorbed in all analyzed flow rates.

As shown in table 4.1, pressure has a major impact on both CO_2 and ethylene absorption. Increasing pressure leads to better absorption properties, with the drawback of higher energy demand in the compression step, as well as increasing the number of stages. Table 4.2 shows a comparison on the demand and stages needed when varying pressures. A pressure of 33 bar is selected for the final process. However, higher pressures could be analyzed to evaluate the methanol required to achieve desired compositions, as well as the impact of pressure in the techno-economic analysis, both in CAPEX and OPEX.

Pressure (bar)	CO_2 removal [%]	H_2S removal [%]	Ethylene removal [%]	Propylene removal [%]
50	99.99	100.00	64.27	99.99
40	99.98	100.00	56.34	99.98
33	99.79	100.00	44.14	99.93
25	90.82	100.00	31.46	99.02
20	75.28	100.00	24.27	95.48
15	57.77	100.00	17.19	83.85
10	38.97	100.00	10.48	59.01

Table 4.1: Effect of pressure on the removal rates of CO_2, H_2S, and light olefins at constant methanol flowrate (1000 kg/h per ton MPW).

Pressure (bar)	Demand (kW)	Stages	kW per Stage
50	99	4	25
40	93	4	23
33	88	4	22
25	81	3	27
20	79	3	26
15	71	3	24
10	60	3	20

Table 4.2: Compressor power demand and distribution across stages at different pressures.

4.2.3 Regeneration Challenges Light Olefins

ASPEN Plus azeotrope search tool was used to understand the behavior of the obtained mixture after the cold methanol absorber, and details can be found in Appendix C. 3 different azeotropes were found, with the most relevant being ethylene-CO_2. Typical methanol absorption processes separate CO_2 in flashing stages, as shown in figure 2.7, being the first stage at 11 bar to separate unwanted compounds such as CO and H_2, and the second one at 5 bar to obtain a pure CO_2 stream. The azeotrope formed between ethylene and CO_2 causes a major problem when using a flash as the unit operation to separate the gases. Different flash pressures where simulated, with ethylene and CO_2 going together in the gas outlet, and are shown in table 4.3. It can be seen that CO_2 goes as a gas. However, ethylene and propylene also go in the gas stream, adding an extra separation step. A different process must be developed to separate the CO_2 fraction from the stream, to be followed by the H_2S separation, and finally by the olefin-methanol separation for methanol reuse. The cold methanol regeneration stage is out of the scope of the research. However, it is a crucial part to develop to understand the feasibility of cold methanol use for the cracked gas cleaning and separation.

Component	**5 bar**	**10 bar**	**15 bar**
CO_2	0.63	0.57	0.51
C_2H_4	0.20	0.26	0.27
C_3H_6	0.09	0.07	0.06
C_2H_6	0.03	0.03	0.04
CH_4	0.02	0.05	0.09
Total	**0.97**	**0.98**	**0.97**

Table 4.3: Flashing gas mass fraction for CO_2 separation after cold methanol absorption.

4.3 Contaminants variation

As shown in table A.3, HCl mass fraction in MPW is 0.73% in a dry basis, with 1.3% of the MPW composition coming from PVC, as shown in table A.2. PVC impact in the MPW feed was analyzed, as well as the impacts that it will have in the cleaning and separation process. Different inlet compositions of PVC were analyzed (wt %) and are shown in table 4.4. Increasing the PVC fraction in the MPW feed leads to higher Cl fractions, therefore increasing the HCl concentration in the cracked gas. Equations in appendix D describe the calculations followed to obtain the new elemental analysis compositions when varying the PVC input.

Component	**Base**	**5%**	**10%**	**15%**	**20%**
Carbon (C)	0.666	0.656	0.642	0.629	0.615
Hydrogen (H)	0.095	0.093	0.090	0.087	0.083
Oxygen (O)	0.143	0.138	0.130	0.123	0.116
Nitrogen (N)	0.005	0.005	0.005	0.004	0.004
Sulfur (S)	0.001	0.001	0.001	0.001	0.001
Chlorine (Cl)	0.007	0.028	0.056	0.084	0.112
Ash	0.083	0.080	0.076	0.072	0.068

Table 4.4: PVC change in MPW feedstock.

Changes in the PVC composition will lead to higher water flowrates needed to remove HCl from the cracked gas in the DCC unit (#2 in figure 3.1), as well as a cooling step to cool down acid water, because of the exothermic nature of HCl absorption. pH control will also be needed to ensure the proper operation of the DCC unit. For NH_3 variation, the same consequences are expected.

Changes in CO_2 and $H2_S$ concentrations will lead to a variation in the methanol demand, controlled by the CO_2 concentration.

4.4 Sizing

This section presents the estimated sizes for the unit operations involved in the process, as well as the fuel requirement to crack plastic waste in the steam cracker with the compositions used [10], to have an approximate size for the DFB based on the energy requirement to crack the feedstock. The sizing calculations assume a production of 11.6 kton ethylene per year, having an input of 12 ton/h MPW, with a lower flowrate of 5.3 ton/h PE, due to its higher ethylene conversion rate and higher carbon content. Table 4.5 shows the sizes calculated for the pressure vessel calculations (using 12 ton MPW/h plastic waste), while table 4.6 shows the obtained values for the pumping and compression requirements. The same equipment size will be used for MPW and PE feedstock, even if the flowrate varies.

The fuel consumption for PE and MPW was also calculated by simulating the required energy to convert the raw materials into the specified product compositions.

Unit Operation	P (bar)	D (m)	H (m)	Wt (mm)	Stages	Reference
DCC	1	1.76	3.00	7	5	[37]
Flash tank	1	1.56	2.45	7	1	[37]
Methanol absorber	33	0.53	11.00	7	18	[37]

Table 4.5: Pressure vessels sizing. P: pressure, D: diameter, H: height, Wt: wall thickness.

Unit Operation	Value	Units	Reference
Methanol pump	18	m3/h	ASPEN
Multi-stage compressor	1060	kW	ASPEN

Table 4.6: Compression and pumping requirements.

For PE, 4MJ/kg are required to convert PE into the specified product compositions, while for MPW 3.2 MJ/kg are required. Considering the flowrates stated for the sizing, a capacity of at least 11 MW for the DFB without considering heat losses is required to meet the production rates specified for both raw materials.

	MPW	**PE**
kg/h	12000	5272
kg/s	3,33	1,46
Ethylene (kg/h)	1608	1608
Fuel (MJ/kg feed)	3,2	4,0
Ethylene (MJ/kg C_2H_4)	23,7	13,1
Energy Demand (MW)	11	6

Table 4.7: Comparison of MPW and PE scenarios in terms of feed, ethylene production, and energy requirements.

4.5 Economic Analysis

This section analyzes the investment and operating costs required to run a 11.6 kton/year ethylene steam cracking plant. A sensitivity analysis discussing the impact of utilities and raw materials is also included. Table 4.8 presents the included products in the analysis, as well as the production rates for each one of them, obtained from the ASPEN Plus simulation.

4.5.1 CAPEX

The CAPEX calculated using sizing values and cost functions from section 3.4.1, table 3.2, is shown in table 4.9, using a factor of 0.15 of total equipment cost for the HEX network. The gasifier and combustion system represents approximately

	PE (kton/y)	MPW (kton/y)
Feed	42.2	96.0
Ethylene	11.6	11.6
Propylene	4.3	5.3
Butadiene	2.7	2.4
Benzene	3.9	5.9
Toluene	1.2	1.8
Styrene	0.6	2.2
Total	**24.3**	**29.1**

Table 4.8: Production rates for economic analysis.

62% of the total CAPEX, followed by the compressors with a 27% share, the heat exchanger network with a 7% share, and the pressurized vessels (DCC, methanol absorption, and flash tank) with less than 4%. A gasification island, comprising a fuel handling system, combustor and gasifier, and flue gas cleaning of 20 MW size was assumed for the CAPEX estimation.

Unit Operation	Cost (MSEK 2024)	Reference
HEX Network	4.0	[37]
DCC	0.4	[37]
Flash tank	0.3	[37]
Methanol absorption tower	0.7	[37]
Compression system	14.8	[37]
Pumps	0.3	[37]
Gasification Island	34.0	[41]
Total plant cost	54.6	
Fixed capital cost	215.7	
Working capital	10.8	

Table 4.9: CAPEX Summary.

4.5.2 OPEX

Fixed operating costs are summarized in table 4.10, with the operation having a total fixed cost of 46.1 MSEK per year. This fixed cost will remain the same for MPW and PE, as there is no re-sizing for PE flowrates.

The variable operating costs for PE and MPW are shown in figure 4.9, considering methanol cost, electricity, steam, refrigeration, and fuel to maintain the boiler working. A total variable OPEX of 29.5 MSEK per year is achieved for ethylene production with PE as the feedstock, while using MPW increases the OPEX by approximately 50%, having a value of 56.5 MSEK per year. Differences between the PE and MPW OPEX comes from the higher flowrates needed when using MPW. As a

Parameter	Cost (MSEK 2024)
Maintenance	7.6
Labor	10.5
Lab cost	0.5
Supervision	2.1
Management	5.2
Rate on capital	12.7
Insurance and taxes	7.5
Total fixed costs	46.1

Table 4.10: Fixed OPEX Summary.

lower ethylene conversion is obtained, more mass is needed, increasing the methanol consumption, refrigeration, and electricity. The steam consumption for CO_2 desorption increases dramatically due to the higher CO_2 concentration in MPW cracked gas. A higher energy demand is also needed, increasing the fuel consumption.

Figure 4.9 shows the variable operating cost in terms of SEK / kg olefin produced for both PE and MPW. As specified in table 4.8, olefins considered for this analysis are ethylene, propylene, and butadiene. The difference in electricity consumption comes from the higher flowrates of gas that MPW steam cracking produces, giving the multi-stage compressor higher energy requirements. Fuel difference comes for the energy requirement in the steam cracker from the different mass of feedstock. Refrigeration and methanol demand also come from dealing with a lower production volume in the process. Finally, the steam considered for CO_2 desorption in the methanol absorption process is noticeably lower in the PE case, as CO_2 production is minimal compared to the MPW case, as can be seen in table A.4. It is important to notice that steam OPEX only considers the CO_2 desorption in the process, and its not considering the energy required to separate H_2S and olefins present in the rich methanol stream.

4.5.3 Sensitivity Analysis

Figure 4.10 shows three different scenarios to predict the uncertainty of the olefin production price in the process, and to obtain a production price range to compare with actual technologies. Base case presents the production price with the actual assumptions, while +50% OPEX increases the operational cost, having a third case increasing by 50% both the OPEX and the CAPEX.

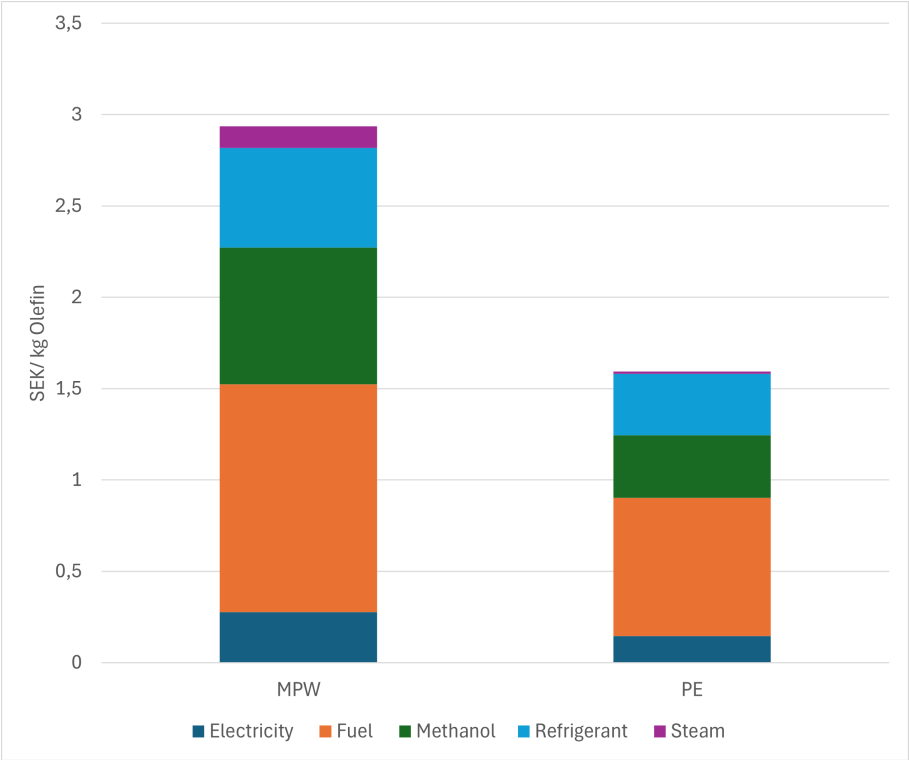

Figure 4.9: Variable OPEX of PE and MPW.

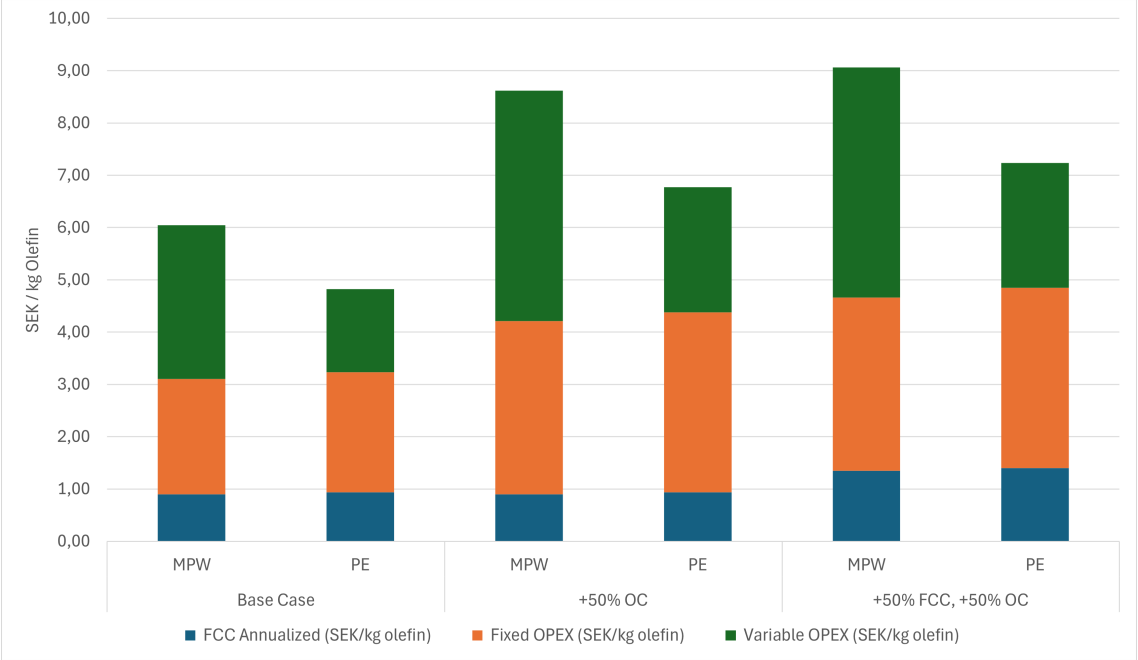

Figure 4.10: Sensitivity Analysis for MPW and PE. Not considering material and sorting cost for MPW and PE.

An olefin production cost ranging from 6 to 9 SEK/kg was obtained when using MPW as feedstock for the process, while the cost ranged from 5 to 7 SEK/kg when

using PE. This costs assume there is no additional fee for the sorting of plastic to obtain a high purity feedstock (as the PE case simulates). An additional scenario is presented in figure 4.11, where the sorting of plastic (in this case PE cost) is considered to be 680 SEK per ton, to match MPW production cost.

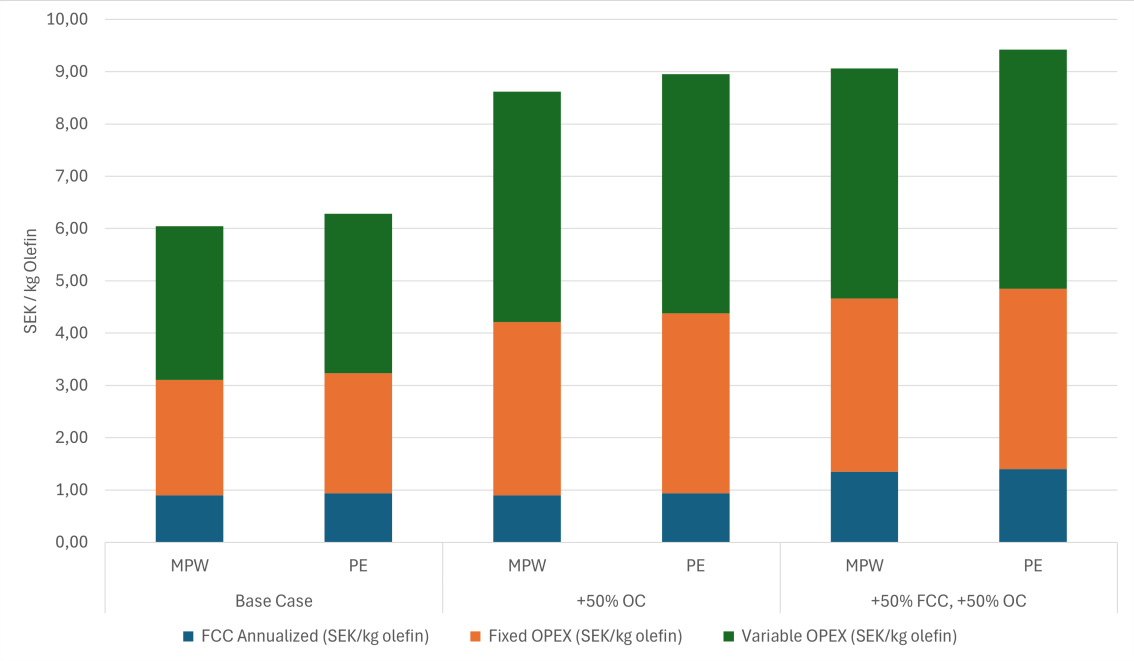

Figure 4.11: Sensitivity Analysis for MPW and PE, considering a sorting cost of 680 SEK/kg for PE.

Including sorting costs is a critical parameter to consider when deciding the feedstock to use in a future process. Sorting processes to obtain higher purity plastic will increase material costs, and therefore increase the OPEX and final cost of SEK/kg olefin. For a case where MPW has no cost, and PE has a cost of 680 SEK/ton, both feedstock show a base price of 6 SEK/kg approximately.

5

Conclusion

The major findings and conclusions from the project are presented in this section.

The process uses the steam cracking gas from two different feedstocks, with a DCC unit to remove PAH and acids (HCl and NH_3), a flash unit to remove excess water, a multi-compression unit to condense BTXS and water, as well as prepare the gas to the next unit, and the cold methanol absorber to remove CO_2 and H_2S while absorbing hydrocarbons. From the simulations in ASPEN Plus, conclusions can be drawn.

Methanol absorption for BTXS removal presents the challenge of dealing with high methanol flowrates, using 3000 kg/h per ton MPW to absorb BTXS and water without a previous water condensation step. Increasing operating pressure from 1 to 10 bar decreases methanol use by 88%. However, regeneration challenges are present due to different azeotropes present in the rich methanol stream, with methanol-water-BTXS streams requiring multi-stage distillation to regenerate methanol.

A compression step increasing pressure up to 33 bar can remove approximately 90% of benzene, 99% of toluene, 99% of styrene, 99% of remaining water, while not having a considerable impact on ethylene and propylene removal (<5%). As the compression system is required for the cold methanol absorption process, this is the best option studied for BTXS separation.

Regarding the cold methanol absorption process, the simulation shows that for complete ethylene absorption methanol flowrates increase up to 4000 kg/h per ton MPW. Using smaller flow rates will lead to ethylene going in the syngas stream. However, if the methanol flowrate is too low, CO_2 absorption will also be affected, having high concentrations in the syngas stream. Pressure also shows an impact on cold methanol absorption, with 33 bar being the base case. Using pressures higher than 33 bar can enhance ethylene absorption and could be studied in further research. As approximately 50% of ethylene is absorbed, the current model will obtain ethylene from 2 streams: syngas and ethylene going to the fractionation plant, and ethylene recovered from the cold methanol regeneration process along with other olefins. The methanol regeneration process and olefin separation simulation is out of the scope of the project. However, major regeneration challenges are the azeotrope formed between CO_2 and ethylene, which will lead to a complicated separation process for

methanol regeneration and olefin separation from contaminants.

From the sizing calculations, the estimated energy demand for both PE and MPW was calculated, assuming a gasification island of 20 MW for the process. From MPW and PE economic evaluation, production costs difference comes from variable OPEX, as PE feedstock is approximately half of MPW to produce the same amount of ethylene. Fuel, methanol, and refrigeration costs are the main drivers of this difference. A final production cost ranging from 6 to 9 SEK/kg olefin was obtained for MPW, with PE giving values of 5 to 7 SEK/kg olefin. It is important to notice that no additional cost for sorting was considered for PE feedstock. An analysis considering this cost shows that sorting could lead to lower feedstock volume, but to higher production costs due to the increase in variable OPEX coming from the sorting cost of a pure plastic stream.

Methanol use for BTXS components gives more challenges than answers to the aromatics removal, due to the high methanol flowrates needed, as well as the complicated regeneration process. For olefins, cold methanol absorption could be a technology to implement if the methanol regeneration process technology is developed in future work, with the possibility of capturing CO_2 coming from the cracked gas. There is uncertainty on the production cost, as the regeneration process was only considered in the sensitivity analysis as 50% increase in CAPEX and OPEX. However, a range from 6 to 10 SEK/kg olefin is useful to understand where the plastic waste steam cracking technology stands when using methanol for acid gas and olefin removal.

The model of a process to remove contaminants and olefins from the plastic waste cracked gas shows encouraging results. Contaminant removal can be handled with a water DCC and methanol absorption system. The absorption of light olefins in a cold methanol absorber shows promising results in terms of efficiency, with ideal process parameters to absorb 100% of olefins in methanol being still an area of opportunity. The process is robust enough to deal with contaminant variation, with solvent flows needed to be adjusted depending on the inlet concentrations.

5.1 Future Work

The next steps of this project would be to investigate the feasibility of separating the cold methanol-CO_2-H_2S-olefin rich stream, the process flow it will follow and the impact that it will have in both the CAPEX and OPEX. Prices on both MPW and PE must be defined for the operating period. Different feedstock, such as pyrolysis oil or textile residues, can also be implemented in the model. Experimental work must be performed to verify the ASPEN Plus results and, if needed, adjust the interaction parameters between methanol and olefins entering the absorption column.

References

1. Geyer R and Jambeck K. Law, Production, use, and fate of all plastics ever made. Sci. Adv. 2017; 3(7). DOI: e1700782
2. OECD. Plastic waste generation worldwide from 1980 to 2019, by application (in million metric tons). Available from: https://www.statista.com/statistics/1339124/global-plastic-waste-generation-by-application/. (accessed: 28.01.2025)
3. Plastics Europe. The Circular Economy for Plastics – A European Analysis 2024. Available from: https://plasticseurope.org/knowledge-hub/the-circular-economy-for-plastics-a-european-analysis-2024/. (accessed: 28.01.2025)
4. Thunman H, Berdugo T, Seemann M, Maric J, Canete I, Pissot S, and Nguyen H. Circular use of plastics-transformation of existing petrochemical clusters into thermochemical recycling plants with 100 percent plastics recovery. Sustainable Materials and Technologies 2019; 22. DOI: https://doi.org/10.1016/j.susmat.2019.e00124
5. Gholami Z, Gholami F, Tisler Z, and Vakili M. A Review on the Production of Light Olefins Using Steam Cracking of Hydrocarbons. Energies 2021; 14:8190. DOI: https://doi.org/10.3390/en1423819
6. Li J et al. Technological progress and coupling renewables enable substantial environmental and economic benefits from coal-to-olefins. Journal of Environmental Management 2024; 353. DOI: https://doi.org/10.1016/j.jenvman.2024.12022
7. Meindersma G. Extraction of aromatics from naphtha with ionic liquids : from solvent development to pilot RDC evaluation. 2005
8. Lee A and Liew M. Tertiary recycling of plastics waste: an analysis of feedstock, chemical and biological degradation methods. Journal of Material Cycles and Waste Management 2024; 43:23–32
9. Praveenkumar T and others. Current technologies for plastic waste treatment for energy recovery, it's effects on poly aromatic hydrocarbons emission and recycling strategies. Fuel 2024; 357. DOI: https://doi.org/10.1016/j.fuel.2023.129379
10. Mandiwala C, Forero R, Berdugo T, Gogolev I, Gonzalez-Arias J, Canete I, Thunman H, and Seemann M. Steam cracking in a semi-industrial dual fluidized bed reactor: Tackling the challenges in thermochemical recycling of plas-

tic waste. Chemical Engineering Journal 2024; 500. DOI: https://doi.org/10.1016/j.cej.2024.156892
11. Kohl A and Nielsen R. Gas Purification. Gulf Professional Publishing, 1997
12. Sun L and Smith R. Rectisol wash process simulation and analysis. Journal of cleaner production 2012; 39:321–8. DOI: http://dx.doi.org/10.1016/j.jclepro.2012.05.049
13. BOREALIS AB. Borealis completes Stenungsund cracker furnace revamp, elevating plant to higher energy efficiency and process safety standards. Available from: https://www.borealisgroup.com/news/borealis-completes-stenungsund-cracker-furnace-revamp-elevating-plant-to-higher-energy-efficiency-and-process-safety-standards. (accessed: 11.03.2025)
14. Sherif A. Integration of a Carbon Capture process in a chemical industry: Case study of a steam cracking plant. Master's Thesis. Chalmers University of Technology 2010
15. Wang Y, Bo Peh S, and Zhao D. Alternatives to Cryogenic Distillation: Advanced Porous Materials in Adsorptive Light Olefin/Paraffin Separations. Small 2019; 15. DOI: https://doi.org/10.1002/smll.201900058
16. Bruce R. Olefin/Paraffin Separation Technology: A Review. Ind. Eng. Chem. Res. 1993; 32:2208–12
17. Gijzel RA van. Energy analysis and plant design for ethylene production from naphtha and natural gas. Eindhoven University of Technology 2017
18. Kermani B, Martin J, and Esaklul K. Materials Design Strategy: Effects of H2S/CO2 Corrosion on Materials Selection. 2006. DOI: https://onepetro.org/NACECORR/proceedings-pdf/CORR06/All-CORR06/NACE-06121/1827108/nace-06121.pdf
19. Alkovali G. Plastic materials: chlorinated polyethylene (CPE), chlorinated polyvinylchloride (CPVC), chlorosulfonated polyethylene (CSPE) and polychloroprene rubber (CR). Toxicity of building materials 2012 :54–75. DOI: 10.1016/B978-0-85709-122-2.50003-6
20. Wadi V, Halique K, and Alhassan S. Polypropylene–Elemental Sulfur (S8) Composites: Effect of Sulfur on Morphological, Thermal, and Mechanical Properties. IEC Research 2020; 59. DOI: https://dx.doi.org/10.1021/acs.iecr.0c01687?ref=pdf
21. Mutlu H and Theato P. Making the Best of Polymers with Sulfur–Nitrogen Bonds: From Sources to Innovative Materials. Macromolecular rapid communications 2020; 41. DOI: https://doi.org/10.1002/marc.202000181
22. Kappler J and others. Sulfur-Composites Derived from Poly(acrylonitrile) and-Poly(vinylacetylene) – A Comparative Study on the Role ofPyridinic and Thioamidic Nitrogen. Batteries and supercaps 2023; 6. DOI: https://doi.org/10.1002/batt.202200522
23. Mandviwala C, González A, Seemann M, and others. . Fluidized bed steam cracking of rapeseed oil: exploring the direct production of the molecular building blocks for the plastics industry. Biomass Conversion and Biorefinery 2023; 13:14511–22. DOI: http://dx.doi.org/10.1007/s13399-022-02925-z

24. Penu O, Dinca C, Slavu N, and Badea A. Effects of advanced cooling of physical solvents in the rectisol process. Proceedings of 2019 International Conference on Energy and Evironment 2019 :54–8. DOI: 10.1109/CIEM46456.2019.8937620
25. Yang S, Zhang L, and Song D. Conceptual design, optimization and thermodynamic analysis of a CO2 capture process based on Rectisol. Energy 2022; 244:69–74. DOI: https://doi.org/10.1016/j.energy.2021.122566
26. Nassar V, Bullin J, and Lyddon L. Solubility of Hydrocarbons in Physical Solvents. Bryan Research Engineering, Inc 2006. DOI: https://www.bre.com/PDF/Solubility-of-Hydrocarbons-in-Physical-Solvents.pdf
27. ASPEN Tech. Aspen Plus. Available from: https://www.aspentech.com/en/products/engineering/aspen-plus. (accessed: 12.05.2025)
28. He J, Shen Y, Li M, et al. The revised PSRK thermodynamic equation and whole process simulation of rectisol. Chemical Engineering 2017; 45:69–74. DOI: DOI:10.3969/j.issn.1005-9954.2017.03.014
29. Iruretagoyena B, Hellgardt K, and Chadwick D. Catalytic systems in the purification of carbon monoxide from hydrogen and ethylene-rich gasses. Master's Thesis. Aalto University. School of Chemical Technology 2023
30. NC STATE. Pumping Plant Performance. Available from: https://content.ces.ncsu.edu/pumping-plant-performance. (accessed: 28.02.2025)
31. Hofbauer H and Rauch R. Stoichiometric Water Consumption of Steam Gasification by the FICFB-Gasification Process. Progress in thermochemical biomass conversion 2001. DOI: https://doi.org/10.1002/9780470694954.ch14
32. Mandviwala C. Steam Cracking in Dual Fluidized Beds: One Step Towards Complete Recyclability of Plastic Waste Using Thermochemical Conversion. Doctoral Thesis. Chalmers University of Technology 2024. DOI: https://research.chalmers.se/en/publication/542360
33. Ganesh S, Göebel H, and Mathias P. Thermodynamic model to study removal of Chlorine, Silicon Tetrafluoride and other uncommon materials from off gases. Chemical Engineering Transactions 2018; 69. DOI: https://www.aidic.it/cet/18/69/055.pdf
34. Atlas Copco. Compressed air manual. Available from: https://www.atlascopco.com/content/dam/atlas-copco/local-countries/united-kingdom/documents/Atlas-Copco-Compressed-Air-Manual-8th-edition.pdf. (accessed: 28.03.2025)
35. Arvidsson M, Morandind M, and Harvey S. Biomass Gasification-Based Syngas Production for a Conventional Oxo Synthesis Plant—Process Modeling, Integration Opportunities, and Thermodynamic Performance. Energy and fuels 2014; 28:4075–87. DOI: https://doi.org/10.1021/ef500366p
36. NORD POOL. Market Data. Available from: https://data.nordpoolgroup.com/auction/day-ahead/prices?deliveryDate=2025-04-23&currency=EUR&aggregation=YearlyAggregate&deliveryAreas=SE3. (accessed: 22.04.2025)
37. Towler G and Sinnot R. Chemical Engineering Design : Principles, Practice and Economics of Plant and Process Design. Elsevier Ltd., 2012
38. Zimmerman H and Walzi R. Ethylene. Encyclopedia of Industrial Chemistry 2001. DOI: https://doi.org/10.1002/9780470694954.ch14

39. Charles Maxwell. Cost Indices: Chemical Engineering Plant Cost Index (CEPCI). Available from: https://toweringskills.com/financial-analysis/cost-indices/. (accessed: 22.04.2025)
40. Roshan T, Matisson T, and Rydén M. Techno-Economic Assessment of Chemical Looping Gasification ofBiomass for Fischer−Tropsch Crude Production with Net-NegativeCO2 Emissions: Part 2. Energy and Fuels 2022; 36:9706–18. DOI: https://doi.org/10.1021/acs.energyfuels.2c01184
41. Thunman H, Gustavsson C, Larsson A, Gunnarsson I, and Tengberg F. Economic assessment of advanced biofuel production via gasification using cost data from the GoBiGas plant. Energy Science and Engineering 2018; 7:217–29. DOI: https://doi.org/10.1002/ese3.271
42. Luyben W. Estimating refrigeration costs at cryogenic temperatures. Computers and Chemical Engineering 2017; 103:144–50. DOI: https://doi.org/10.1016/j.compchemeng.2017.03.013
43. Lux Research. Future of methanol: The cost of moving away from natural gas. Available from: https://luxresearchinc.com/blog/future-of-methanol-the-cost-of-moving-away-from-natural-gas/. (accessed: 22.04.2025)
44. Fortet J and Chehade Y. Feasibility study of implementing Chemical Looping Combustion with BECCS. Master's Thesis. Chalmers University of Technology 2023
45. Sandrameli SM. Thermal/catalytic cracking of hydrocarbons for the production of olefins: A state-of-the-art review I: Thermal cracking review. Fuel 2015; 140:102–15. DOI: http://dx.doi.org/10.1016/j.fuel.2014.09.034

A

Appendix 1

A.1 Naphtha cracking conventional product compositions

Feedstock	1	2	3	4	5	6	7	8	9	10
H_2	1	0.5	4.2	4.1	1.4	0.8	0.9	0.4	1	0.4
CH_4	15	16	5.4	5.1	25.7	25.8	13.6	13.8	14.9	15
C_2H_6	3.9	5.3	32.7	34.1	4.3	6.5	4.3	4	3.4	6.5
C_2H_4	25.7	27.4	49.7	49.2	33.2	32.7	26.8	25.4	27.2	28.2
C_2H_2	0.4	0.6	0.4	1.2	0.8	0.9	0.5	0.5	0.8	0.4
C_3H_8	0.7	1.5	0.9	0.7	2.9	3.5	0.4	0.4	0.4	0.7
C_3H_6	13.5	13.7	15	13.9	14	14.2	15.6	15.6	17	16.4
C_3H_4	0.8	0.8	0.1	0	1	1.1	0.7	0.7	1	0.6
C_4H_{10}	0.3	0.4	0.6	0.3	1.2	0.4	0.4	0.4	0.3	0.4
C_4H_8	3.7	3.1	0.3	0	2.7	3.4	5.2	4.3	5.1	4.3
C_4H_6	5.2	4.7	2	2.9	3.4	2.5	5.9	5.6	7	5.9
Benzene	9	8.8	5.4	5.3	9	6.4	7.6	8.2	6.4	4.1
Toluene	4.9	4.8	4.1	4	2.2	1.4	4.4	4.6	3.2	3.9
Xylenes	1.1	0.7	0.1	0	0.1	1.3	1.4	1.4	1	0.4
Ethylbenzene	0	0	0	0	0	0.1	0.3	0.2	0	0
Styrene	1.3	0.4	0.1	0	0.5	0.1	1	0.4	1.5	1.2
C_5	3.5	3.6	2.5	2.6	2.3	2.2	4.3	4	4.8	6
C_6	2.1	2.2	0.2	0.1	0.8	0.8	3	2.4	2.5	3.5
C_7^+	6.8	6.7	0.1	0.5	1.6	2	5.6	6.2	6.1	6
Total	98.9	101.2	123.8	124	107.1	106.1	101.9	98.5	103.6	103.9

Table A.1: Cracking product composition in a conventional steam cracking furnace. (1, 6-10 Naphtha feedstock) Adapted from [45]

A.2 Dual fluidized bed reactor fuel characterization

Feedstock	PE + PP	Cellulose	PS	PET	PVC	PA
%weight. of dry feedstock						
MPW	45.80	20.90	9.32	10.12	1.30	4.20

Table A.2: Composition of Municipal Plastic Waste (MPW) by polymer type

Component	Naphtha	PE	MPW	CRR	MRP	Pyrolysis oil
Moisture (%wt of feedstock)						
Moisture	0	0	3.5	4.5	0	0
Elemental composition (%wt dry basis)						
Carbon (C)	84.11	85.7	66.6	60.6	85.26	85.63
Hydrogen (H)	15.88	14.2	9.5	8.8	14.12	14.35
Oxygen (O)	0	0	14.27	21	0	0
Nitrogen (N)	0	0	0.52	0.35	0.01	0
Sulfur (S)	0	0	0.08	0.07	0.01	0
Chlorine (Cl)	0	0	0.73	0.2	0.1	0
Ash	0	0.08	8.29	8.75	0.1	0
Total	**99.99**	**99.98**	**99.99**	**99.77**	**99.6**	**99.98**

Table A.3: Elemental composition of different feedstocks entering the DFB steam cracking process. Adapted from [10]

A.3 Dual fluidized bed reactor steam cracking product compositions

Parameter	Naphtha	PE	MPW	CRR	MRP	Pyrolysis oil
Temperature (°C)	782	783	768	742	789	755
Feeding rate (kg/h)	40	90	50	50	100	28
Hydrogen (H_2)	0.016	0.011	0.011	0.012	0.01	0.01
Carbon monoxide (CO)	0.045	0.017	0.064	0.107	0.021	0.03
Carbon dioxide (CO_2)	0.176	0.08	0.31	0.306	0.066	0.085
Methane (CH_4)	0.149	0.122	0.079	0.075	0.137	0.124
Ethylene (C_2H_4)	0.305	0.304	0.134	0.131	0.288	0.238
Ethane (C_2H_6)	0.02	0.037	0.018	0.02	0.06	0.027
Propylene (C_3H_6)	0.141	0.112	0.061	0.076	0.126	0.123
Propane (C_3H_8)	0.008	0.008	0.004	0.013	0.008	0.008
1,3-Butadiene (C_4H_6)	0.046	0.064	0.025	0.036	0.047	0.053
1-Butene (C_4H_8)	0.0106	0.0132	0.0011	0	0.0065	0.0184
Isobutylene (C_4H_8)	0.0191	0.0005	0.0078	0.0104	0.0198	0.0107
C5 Olefins (C_5H_8)	0.023	0.0157	0.006	0.006	0.01	0.006
Benzene (C_6H_6)	0.049	0.104	0.068	0.055	0.115	0.039
Toluene ($C_6H_5CH_3$)	0.007	0.032	0.021	0.017	0.044	0.016
Styrene (C_8H_8)	0.004	0.016	0.025	0.012	0.018	0.016
PAHs ($C_{10}H_8$)	0.007	0.034	0.027	0.018	0.042	0.016
Solid carbon (C)	0.005	0.0236	0.0231	0.0394	0.0262	0.005
Total (kg/kg dry stock)	1.0257	0.994	0.885	0.9338	1.0445	0.8201

Table A.4: DFB Steam cracking product yields (kg/kg dry stock). Adapted from [10]

Component	**Formula**	**Naphtha**	**PE**	**MPW**	**CRR**	**MRP**	**Pyrolysis Oil**
Carbon monoxide	CO	0.0301	0.0115	0.0459	0.0779	0.0143	0.0201
Carbon dioxide	CO_2	0.1177	0.0542	0.2224	0.2229	0.0448	0.0569
Methane	CH_4	0.0997	0.0827	0.0567	0.0546	0.0930	0.0829
Ethylene	C_2H_4	0.2040	0.2060	0.0961	0.0954	0.1955	0.1592
Ethane	C_2H_6	0.0134	0.0251	0.0129	0.0146	0.0407	0.0181
Propylene	C_3H_6	0.0943	0.0759	0.0438	0.0553	0.0856	0.0823
Propane	C_3H_8	0.0054	0.0054	0.0029	0.0095	0.0054	0.0054
1,3-butadiene	C_4H_6	0.0308	0.0434	0.0179	0.0262	0.0319	0.0355
1-butene	C_4H_8	0.0071	0.0089	0.0008	0.0000	0.0044	0.0123
Isobutylene	C_4H_8	0.0128	0.0003	0.0056	0.0076	0.0134	0.0072
C5 olefins	C_5H_x	0.0154	0.0106	0.0043	0.0044	0.0068	0.0040
Benzene	C_6H_6	0.0328	0.0705	0.0488	0.0401	0.0781	0.0261
Toluene	C_7H_8	0.0047	0.0217	0.0151	0.0124	0.0299	0.0107
Xylene	C_8H_{10}	0.0027	0.0108	0.0179	0.0087	0.0122	0.0107
PAHs	PAHs	0.0047	0.0230	0.0194	0.0131	0.0285	0.0107
Hydrogen Sulfide	H_2S	0.0000	0.0000	0.0006	0.0005	0.0001	0.0000
Ammonia	NH_3	0.0000	0.0000	0.0044	0.0030	0.0001	0.0000
Hydrochloric Acid	HCl	0.0000	0.0000	0.0052	0.0014	0.0007	0.0000
Water	H_2O	0.3139	0.3424	0.3715	0.3437	0.3077	0.4514
Hydrogen	H_2	0.0107	0.0075	0.0079	0.0087	0.0068	0.0067
Total		1.0000	1.0000	1.0000	1.0000	1.0000	1.0000

Table A.5: ASPEN Inlet Mass Fractions of Components in Different Streams

Table A.6: Product yields and operating conditions for PE and MPW

Parameter	**PE**	**MPW**
Temperature (°C)	783	768
Feeding rate (kg/h)	90	50
Hydrogen (H_2)	0.011	0.011
Carbon monoxide (CO)	0.017	0.064
Carbon dioxide (CO_2)	0.080	0.310
Methane (CH_4)	0.122	0.079
Ethylene (C_2H_4)	0.304	0.134
Ethane (C_2H_6)	0.037	0.060
Propylene (C_3H_6)	0.112	0.061
Propane (C_3H_8)	0.008	0.004
1,3-Butadiene (C_4H_6)	0.064	0.025
1-Butene (C_4H_8)	0.0132	0.0011
Isobutylene (C_4H_8)	0.0005	0.0067
C5 Olefins (C_5H_8)	0.0157	0.006
Benzene (C_6H_6)	0.104	0.068
Toluene ($C_6H_5CH_3$)	0.032	0.021
Styrene (C_8H_8)	0.054	0.014
PAHs ($C_{10}H_8$)	0.036	0.027
Solid carbon (C)	0.0236	0.0231
Total (kg/kg dry stock)	0.994	0.885

B

Appendix 2

B.1 ASPEN Plus Design Results

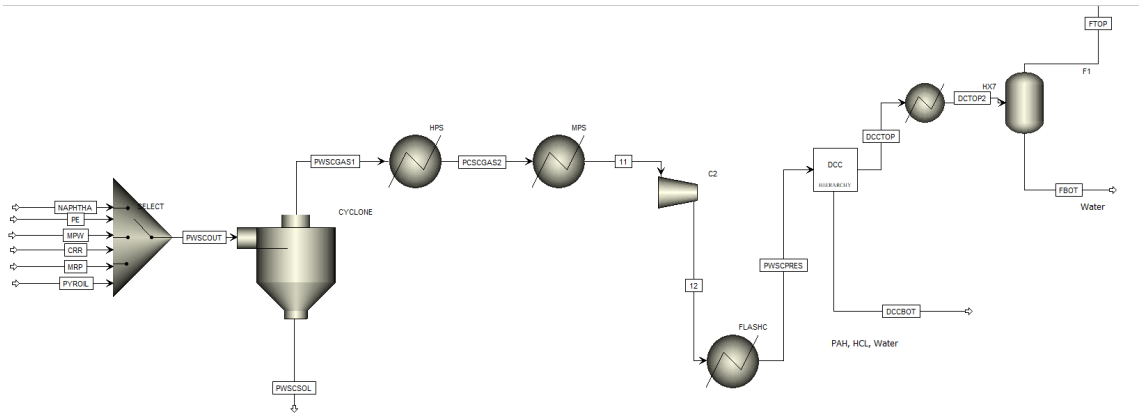

Figure B.1: ASPEN plus sheet part 1.

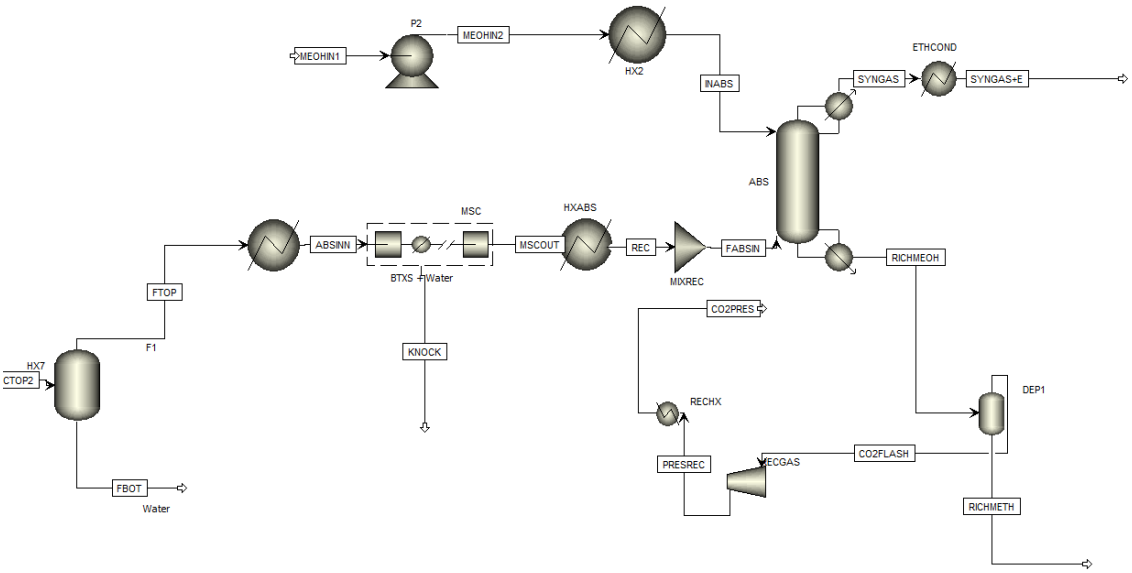

Figure B.2: ASPEN plus sheet part 2.

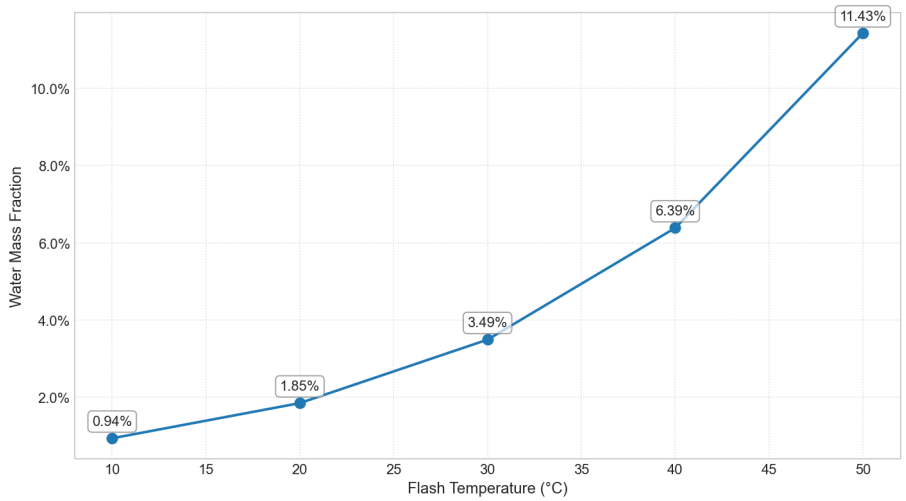

Figure B.3: Flash condenser sensitivity analysis.

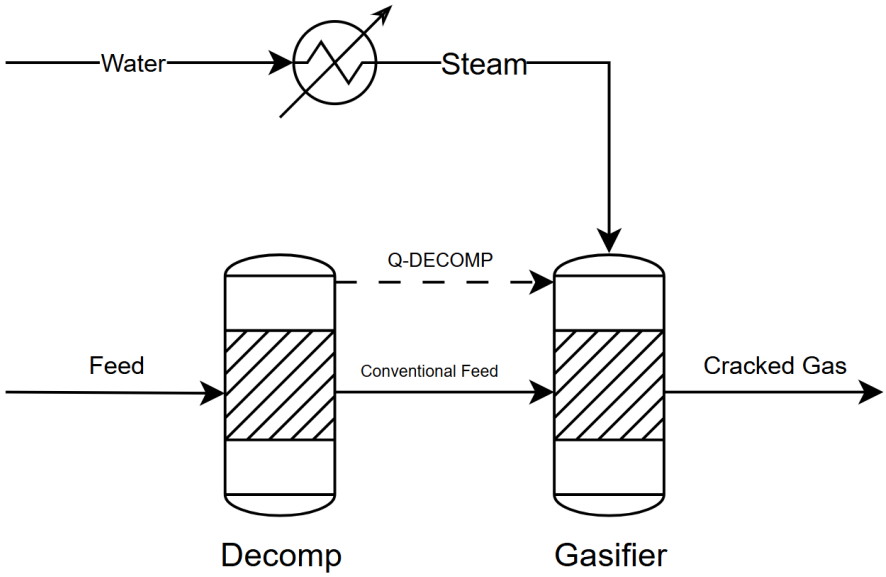

Figure B.4: Gasification energy process diagram.

C

Appendix 3

C.1 Methanol Regeneration Challenges

AZEOTROPE SEARCH REPORT

Physical Property Model:NRTL **Valid Phase:**VAP-LIQ

Mixture Investigated For Azeotropes At A Pressure Of 1 BAR

Comp ID	Component Name	Classification	Temperature
BENZENE	BENZENE	Saddle	79,37 C
TOLUENE	TOLUENE	Saddle	110,21 C
XYLENE	O-XYLENE	Stable node	143,92 C
METHANOL	METHANOL	Saddle	64,31 C
WATER	WATER	Stable node	101,08 C

7 Azeotropes found

01	Number Of Components: 2		Temperature 64,10 C
	Homogeneous		Classification: Unstable node
		MOLE BASIS	MASS BASIS
	BENZENE	0,0871	0,1888
	METHANOL	0,9129	0,8112

02	Number Of Components: 3		Temperature 66,54 C
	Homogeneous		Classification: Saddle
		MOLE BASIS	MASS BASIS
	BENZENE	0,3747	0,6400
	METHANOL	0,3708	0,2598
	WATER	0,2545	0,1003

03	Number Of Components: 2		Temperature 64,37 C
	Homogeneous		Classification: Unstable node
		MOLE BASIS	MASS BASIS
	BENZENE	0,4547	0,7834
	WATER	0,5453	0,2166

04	Number Of Components: 2	Temperature 71,00 C
	Homogeneous	Classification: Saddle

		MOLE BASIS	MASS BASIS
	TOLUENE	0,2898	0,6760
	WATER	0,7102	0,3240

05	Number Of Components: 3		Temperature 72,17 C
	Homogeneous		Classification: Saddle
		MOLE BASIS	MASS BASIS
	TOLUENE	0,2422	0,5652
	METHANOL	0,2504	0,2032
	WATER	0,5074	0,2315

06	Number Of Components: 2		Temperature 77,35 C
	Homogeneous		Classification: Saddle
		MOLE BASIS	MASS BASIS
	XYLENE	0,2017	0,5982
	WATER	0,7983	0,4018

07	Number Of Components: 3		Temperature 77,58 C
	Homogeneous		Classification: Saddle
		MOLE BASIS	MASS BASIS
	XYLENE	0,1838	0,5468
	METHANOL	0,1049	0,0942
	WATER	0,7113	0,3591

AZEOTROPE SEARCH REPORT

Physical Property Model:NRTL **Valid Phase:**VAP-LIQ

Mixture Investigated For Azeotropes At A Pressure Of 11 BAR

Comp ID	Component Name	Classification	Temperature
CARBONMO	CARBON-MONOXIDE	Unstable node	-162,67 C
CARBONDI	CARBON-DIOXIDE	Saddle	-37,23 C
METHANE	METHANE	Saddle	-122,05 C
ETHYLENE	ETHYLENE	Saddle	-48,93 C
ETHANE	ETHANE	Saddle	-28,96 C
PROPYLEN	PROPYLENE	Saddle	22,82 C
BUTADIEN	1,3-BUTADIENE	Saddle	77,45 C
BENZENE	BENZENE	Stable node	184,17 C
METHANOL	METHANOL	Saddle	139,34 C
H2S	HYDROGEN-SULFIDE	Saddle	2,26 C

3 Azeotropes found

01	Number Of Components: 2		Temperature -49,46 C
	Homogeneous		Classification: Saddle
		MOLE BASIS	MASS BASIS
	CARBONDI	0,1838	0,2610
	ETHYLENE	0,8162	0,7390

02	Number Of Components: 2		Temperature -44,45 C
	Homogeneous		Classification: Saddle
		MOLE BASIS	MASS BASIS
	CARBONDI	0,6274	0,7114
	ETHANE	0,3726	0,2886

03	Number Of Components: 2		Temperature -29,04 C
	Homogeneous		Classification: Saddle
		MOLE BASIS	MASS BASIS

	ETHANE	0,9426	0,9354
	H2S	0,0574	0,0646

D

Appendix 4

D.1 Contaminant Variation Calculations

$$M = \text{Total mass (\%)} \tag{D.1}$$

$$\text{Initial plastic waste} = \text{MPW}_m \tag{D.2}$$

$$\text{Waste w/o PVC} = \text{MPW}_m - \text{PVC}_m \tag{D.3}$$

$$\text{PVC in waste \%} = \left(\frac{\text{PVC}_m}{\text{MPW}_m}\right) \times 100 \tag{D.4}$$

$$\text{Cl}_{\text{MW}} = 35.433 \text{ g/mol} \tag{D.5}$$

$$\text{PVC}_{\text{MW}} = 61.49 \text{ g/mol} \tag{D.6}$$

$$\text{Cl \% in PVC} = 57\% \tag{D.7}$$

$$\text{PVC mass} = \text{PVC}_m \tag{D.8}$$

$$\text{Cl \% in MPW} = 0.73\% \tag{D.9}$$

$$\text{Cl in MPW} = \text{MPW}_m \times \text{Cl\% in MPW} \tag{D.10}$$

$$\text{Cl from PVC} = \text{PVC}_m \times \text{Cl\% in PVC} \tag{D.11}$$

$$\text{Total Cl}_m = \text{Cl in MPW}_m + \text{Cl in PVC}_m \tag{D.12}$$

$$\text{New Cl fraction} = \frac{\text{Total Cl}_m}{\text{Total mass } (M)} \tag{D.13}$$

DEPARTMENT OF EARTH, SPACE AND ENVIRONMENT
CHALMERS UNIVERSITY OF TECHNOLOGY
Gothenburg, Sweden
www.chalmers.se

CHALMERS
UNIVERSITY OF TECHNOLOGY